Towards a theory of wavefunction collapse Part 2:

Collapse as abrupt reconfigurations of wavefunction's evolution in a dynamically expanding spacetime

Garrelt Quandt-Wiese [1]
Schlesierstr. 16, 64297 Darmstadt, Germany
garrelt@quandt-wiese.de
http://www.quandt-wiese.de

arXiv:1701.01765v3 [quant-ph] 1 Feb 2017

A new approach to wavefunction collapse is proposed. The so-called Dynamical Spacetime approach enhances semiclassical gravity and enables it for an explanation of wavefunction collapse by postulating that the spacetime region on which quantum fields exist and on which the wavefunction's evolution can be regarded is bounded towards the future by a spacelike hypersurface, which is dynamically expanding towards the future. Collapse is displayed in the way that the wavefunction's evolution becomes unstable at certain critical expansions of spacetime, at which it reconfigures via a self-reinforcing mechanism quasi-abruptly to an evolution resembling a classical trajectory. Thereby, spacetime geometry changes in favour of the winning state, which causes the path of the other state to vanish by destructive interference. This mechanism for collapse can explain the quantum correlations in EPR experiments without coming into conflict with relativity and the Free Will theorem. The Dynamical Spacetime approach is mathematically formulated on basis of the Einstein-Hilbert action and predicts for the Newtonian limit the same lifetimes of superpositions as the gravity-based approaches of Diósi and Penrose. A second important feature of the Dynamical Spacetime approach is its capability to forecast reduction probabilities. It can explain why all experiments performed so-far confirm Born's rule, and predict deviations from it, when solids evolve into three-state superpositions. The basics needed for the derivations in this paper are developed in Part 1 by an analysis of semiclassical gravity.

Keywords: *Wavefunction collapse, semiclassical gravity, quantum mechanics and relativity, Born's rule, superluminal signalling*.

1 Introduction

A theory for the collapse of wavefunction is one of the most important open issues of physics. It took roughly 30 years from the development of quantum theory in the 1920s until David Bohm addressed the macro-objectification problem of quantum theory for the first time in a consistent model, Bohmian mechanics [5, 6], and it took a further

[1] My official last name is Wiese. For non-official concerns, my wife and I use our common family name: Quandt-Wiese.

30 years until Philip Pearle [7, 8] and Giancarlo Ghirardi [9, 10] addressed in their pioneering works in the 1980s collapse's stochastic nature in consistent models, the dynamical reduction models [28], with help of stochastic differential equations. Beside these models, which focus on describing collapse rather than explaining it, attempts have been made to find the physical origin of collapse. Here gravity is the most often discussed candidate; an idea that had already been mentioned by Richard Feynman in the 1960s [11] and became concrete with the models of Lajos Diósi [12] and Roger Penrose [13] in the 1980s and 1990s. Diósi assumes fluctuations of the gravitational field as the driver of collapse; Penrose the uncertainty of location in spacetime, which occurs when superposed states prefer due to different mass distributions differently curved spacetimes. Interestingly, both approaches predict the same lifetimes of superpositions, which can be calculated with a simple rule of thumb, which sometimes is referred to as the Diósi-Penrose criterion, and which is often used for quantitative assessments of experimental proposals investigating certain properties of wavefunction collapse [14–21].

One of the greatest challenges of collapse models is to make them compatible with relativity. This is due to the deep and troubling conflict between the empirically verified non-local nature of quantum theory in the form of quantum correlations violating Bell's inequalities and the notion of local causality that is motivated by relativity. Relativistic models were developed for Bohmian mechanics [22–27] and the dynamical reduction models [28–37]. For the gravity-based approaches of Diósi and Penrose, relativistic formulations are still missing. An important stimulus for the assessment of relativistic collapse models came from the Free Will theorem of John Conway and Simon Kochen in 2006 [38, 39] showing that in special EPR experiments with free choice of measurements (in the sense that the choices are not functions of the past), information about the choices must travel infinitely fast between the measurement partners. Whether this really implies that there can be no relativistic collapse theory has led to an intensive scientific debate [40–43].

The Dynamical Spacetime approach to wavefunction collapse developed in this paper is, as the approaches of Diósi and Penrose, a gravity-based approach. It is based on semiclassical gravity, in which the gravitational field is not quantised and spacetime geometry is treated classically. A collapse mechanism follows from the fact that the superposed states must share in semiclassical gravity the same classical spacetime geometry, even if they prefer (according to general relativity) differently curved spacetimes, which is the case when their mass distributions are different. This leads to a competition between the states for the curvature of spacetime. However, semiclassical gravity alone cannot explain collapse, which is known from studies of the Schrödinger-Newton equation to display semiclassical gravity in the Newtonian limit.

The Dynamical Spacetime approach to wavefunction collapse enhances semiclassical gravity by postulating that the spacetime region on which quantum fields exist and on which the wavefunction's evolution can be regarded is bounded towards the future by a spacelike hypersurface, which is dynamically expanding towards the future. This

postulate allows for fundamental new behaviour in the way that the wavefunction's evolution can change to a new evolution when spacetime expands. It leads to a collapse mechanism in which the wavefunction's evolution becomes unstable at certain critical expansions of spacetime, at which it reconfigures via a self-reinforcing mechanism quasi-abruptly to an evolution resembling a classical trajectory. This mechanism displays the empirically verified non-local nature of quantum theory and complies with the Free Will theorem and the notion of local causality of relativity as well.

The derivation of the Dynamical Spacetime approach in this paper is prepared by an analysis of semiclassical gravity in Part 1 [1]. A study of Part 1 is not essential.

—

The remainder of this paper is structured as follows. In Section 2, we define the physical approach of our collapse models. In Section 3, we derive the collapse mechanism first for two-state superpositions in the Newtonian limit. In Sections 4 and 5, we generalise the derivation for the relativistic case and show in Section 6 how the quantum correlations in EPR experiments can be explained. In Section 7, we come to the second important feature of the Dynamical Spacetime approach: its capability to forecast reduction probabilities, and derive Born's rule first for two-state superpositions.

In Section 8, we convert our reduction model into a more formal mathematical form and generalise it for superpositions of more than two states. In Section 9, we show why all experiments performed so far behave in accordance with Born's rule with the help of a property that these experiments have in common. This leads us to the investigation of new regimes in Section 10, where we show that the Dynamical Spacetime approach predicts deviations from Born's rule, when solids evolve into three-state superpositions. In Section 11, we discuss the physical consequences resulting from deviations from Born's rule. In Sections 12 and 13, we discuss further aspects of the Dynamical Spacetime approach, such as energy conservation and ontology. The paper ends with an outlook towards Dynamical Spacetime theory in Section 14.

In [2], a quick overview on the derivation and the proposed experimental verification of the Dynamical Spacetime approach is given.

2 Approach

In this section, we define the physical approach of the Dynamical Spacetime approach to wavefunction collapse. The Dynamical Spacetime approach is based on two assumptions: semiclassical gravity and the so-called *Dynamical Spacetime postulate*.

Semiclassical gravity
In semiclassical gravity, the gravitational field is not quantised and spacetime geometry is treated classically [44, 45]. As a consequence, superposed states must share the same classical spacetime geometry, even if they prefer (according to general relativity) differently curved spacetimes, which is the case when their mass distributions are different. This provokes a competition between the states for the curvature of spacetime, which is the driver of collapse in the Dynamical Spacetime approach. However, semiclassical gravity alone cannot explain collapse, which is known from studies of the Schrödinger-Newton equation to display semiclassical gravity in the Newtonian limit [46, 47].

The question of whether the gravitational field must be quantised or not, as assumed by semiclassical gravity, is still the subject of scientific debate [48, 49] and is an issue that has not been decided by experiments so far [50].

Dynamical Spacetime postulate
The Dynamical Spacetime approach postulates that the spacetime region on which quantum fields exist and on which the wavefunction's evolution can be regarded is bounded towards the future by a spacelike hypersurface, the so-called *spacetime border* $\bar{\sigma}$, which is dynamically propagating towards the future over the so-called *dynamical parameter* $\bar{\tau}$, as illustrated in Figure 1. The dynamical parameter itself is not an observable quantity (beable [51]), and can be chosen to be dimensionless. This postulate enables a fundamental new behaviour in the way that the wavefunction's evolution on spacetime can retroactively change to a new evolution, when spacetime expands over $\bar{\tau}$. This is possible, since the wavefunction's evolution is not governed by unitary evolution only, but must in addition satisfy a boundary condition on the spacetime border.

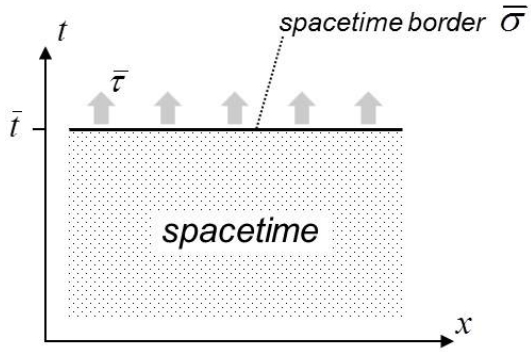

Fig. 1: *Dynamical Spacetime postulate:* Spacetime is bounded towards the future by a spacelike hypersurface, the spacetime border $\bar{\sigma}$, which is dynamically expanding towards the future over the dynamical parameter $\bar{\tau}$.

3 Collapse mechanism for two-state superpositions in the Newtonian limit

In this section, we show how the physical approach defined in Section 2 leads to a mechanism for wavefunction collapse. We restrict our derivation first to two-state superpositions in the Newtonian limit.

Aligning spacetime border's propagation with the experiment's rest frame
Most predictions of the Dynamical Spacetime approach are fortunately not sensitive to the concrete propagation of the spacetime border $\bar{\sigma}(\bar{\tau})$. Discussions, such as the one in this section, can be simplified by assuming that the spacetime border propagates in coincidence with the experiment's rest frame. The spacetime border is then given by a plane hypersurface, which is specified by a point in time $\bar{t}$ in this rest frame; and the dynamical parameter $\bar{\tau}$ can be expressed by this point in time $\bar{t}$ (i.e. $\bar{\tau}\rightarrow\bar{t}$). This is very convenient for the analyses, since spacetime then simply ends at $\bar{t}$, as illustrated in Figure 1.

Abrupt reconfigurations of wavefunctions' evolutions
We start our derivation of the collapse mechanism by presenting its result, i.e. when and how the wavefunction's evolution reconfigures. The mechanism will be derived in the next section.

Our illustration of how the wavefunction's evolution reconfigures refers to the single-photon experiment in the left-hand side of Figure 2, in which a single photon is split by a beam splitter and measured by the detector on the right. For photon detection, the detector displaces the position of a rigid body. This experiment generates a superposition of two states ($|\psi>=c_1|\psi_1>+c_2|\psi_2>$, $|c_1|^2+|c_2|^2=1$) with mass distributions $\rho_1(\mathbf{x})$

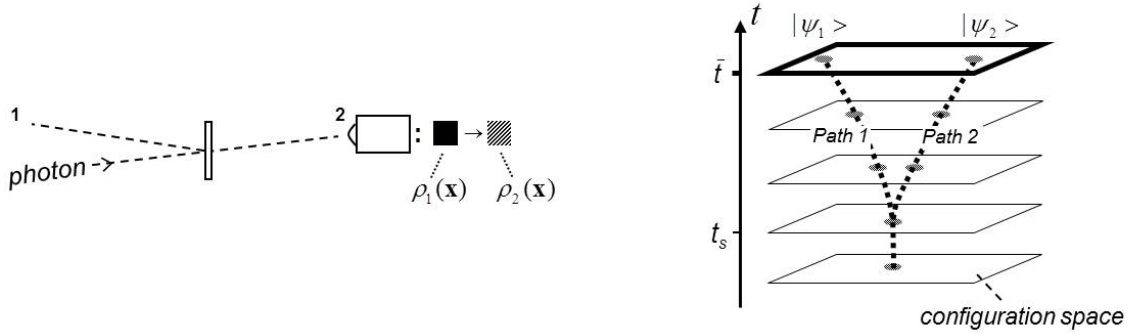

Fig. 2: *Left:* Experiment to generate a superposition of states with mass distributions $\rho_1(\mathbf{x})$ and $\rho_2(\mathbf{x})$. The detector displaces the rigid body for photon detection.
Right: Illustration of the experiment's state vector's evolution in configuration space, which splits into two wavepackets at t_s when the photon enters the beam splitter.

and $\rho_2(\mathbf{x})$, as indicated in the figure. In the right-hand side of the figure, the evolution of the experiment's state vector $|\psi(t)>$ in configuration space is visualised. At time t_s, when the photon enters the beam splitter, the root wavepacket splits into two well separated wavepackets $|\psi_1>$ and $|\psi_2>$. In our discussion, the state vector $|\psi>$ shall always describe the complete system, consisting here of the photon, the beam splitter, the detector and the rigid body.

The critical position of the spacetime border $\bar{\tau}_C$, at which the wavefunction's evolution becomes unstable for reconfiguration and collapses, can be expressed for our special alignment of spacetime border's propagation by a point in time in the experiment's rest frame, the reduction point in time $\bar{t}_C$. This point in time is achieved when the so-called *competition action* between Path 1 and Path 2 in Figure 2 $S_{G12}(\bar{t})$ reaches Planck's quantum of action:

$$S_{G12}(\bar{t}_C) = \hbar \ . \qquad \textit{reduction condition} \tag{1}$$

The competition action between Path 1 and Path 2 $S_{G12}(\bar{t})$ is defined by integrating the characteristic energy of the Diósi-Penrose criterion between the states of the paths E_{G12}, which we call the *Disi-Penrose energy* from the time t_s, when the states $|\psi_1>$ and $|\psi_2>$ are generated until the spacetime border at $\bar{t}$ as follows:

$$S_{G12}(\bar{t}) \equiv \int_{t_s}^{\bar{t}} dt E_{G12}(t) \ . \qquad \textit{competition action} \tag{2}$$

The Diósi-Penrose energy between States 1 and 2 E_{G12} is defined by the integral over the difference of the states' mass distributions $\rho_1(\mathbf{x})-\rho_2(\mathbf{x})$ multiplied by the difference of their gravitational potentials $\Phi_1(\mathbf{x})-\Phi_2(\mathbf{x})$ resulting from these mass distributions [2] as follows [1] [3]:

$$E_{G12} = \frac{1}{2}\int d^3\mathbf{x}(\rho_1(\mathbf{x})-\rho_2(\mathbf{x}))(\Phi_2(\mathbf{x})-\Phi_1(\mathbf{x})) \ . \qquad \textit{Diósi-Penrose energy} \tag{3}$$

The upper part of Figure 3 shows how the wavefunction's evolution reconfigures in configuration space at the reduction point in time $\bar{t}_C$. Here the wavefunction's evolution abruptly reconfigures either completely to Path 1 or Path 2, as shown in the figure. This means that the photon that was split before the reconfiguration by the beam splitter is then either completely reflected or transmitted by it, as illustrated in the lower part of Figure 3. This is the fundamentally new behaviour of the Dynamical Spacetime

[2] $\Phi_i(\mathbf{x}) = -G\int d^3\mathbf{y}\frac{\rho_i(\mathbf{y})}{|\mathbf{x}-\mathbf{y}|}$.

[3] The Diósi-Penrose energy can be written in the better-known form:

$$E_{G12} = \frac{1}{2}G\int d^3\mathbf{x}d^3\mathbf{y}\frac{(\rho_1(\mathbf{x})-\rho_2(\mathbf{x}))(\rho_1(\mathbf{y})-\rho_2(\mathbf{y}))}{|\mathbf{x}-\mathbf{y}|} \ .$$

The factor ½ in this expression is lacking in the original derivations of Diósi [52] and Penrose [13]. In [1], it is shown how this factor can be derived from the approaches of Diósi and Penrose, and from semiclassical gravity (being the basis of the Dynamical Spacetime approach) as well.

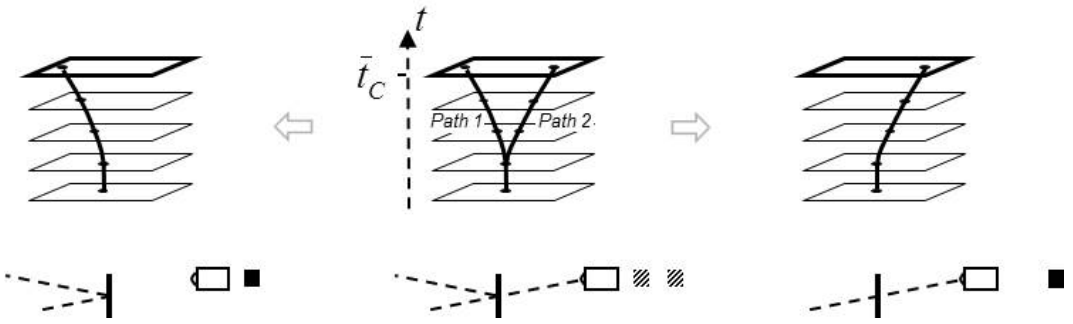

Fig. 3: *Above:* Abrupt reconfiguration of the wavefunction's evolution in configuration space, when the spacetime border reaches the reduction position $\bar{t}_C$.
Below: Corresponding behaviour in spacetime. After reconfiguration, the photon is either completely reflected or transmitted by the beam splitter.

approach that the wavefunction's evolution can retroactively change when spacetime expands.

When the Diósi-Penrose energy $E_{G12}(t)$ is approximately constant over time after the states have split at t_s, the reduction condition (Equation 1) leads to the following reduction point in time:

$$\bar{t}_C \approx \frac{\hbar}{E_{G12}} \quad , \qquad \textit{Diósi-Penrose criterion} \tag{4}$$

which is identical to the lifetime of the superposition predicted by the gravity-based approaches of Diósi and Penrose [13, 52].

Derivation of the collapse mechanism

How the abrupt reconfigurations of wavefunctions' evolutions can be derived from the assumptions of the Dynamical Spacetime approach, semiclassical gravity and the Dynamical Spacetime postulate, will now be explained in three steps.

Step 1: Mutual detuning of the paths

In the Newtonian limit, the sharing of spacetime (semiclassical gravity) is synonymous with the sharing of a common gravitational potential by the states, since the g_{00}-component of the metric field (which is the only relevant one in this limit) can be expressed by the gravitational potential Φ via the relation $g_{00} \approx 1 + 2\Phi/c^2$ [53]. In semiclassical gravity, the common gravitational potential is given by the mean of the states' gravitational potentials [1] by

$$\Phi(\mathbf{x}) = |c_1|^2 \Phi_1(\mathbf{x}) + |c_2|^2 \Phi_2(\mathbf{x}) \quad , \tag{5}$$

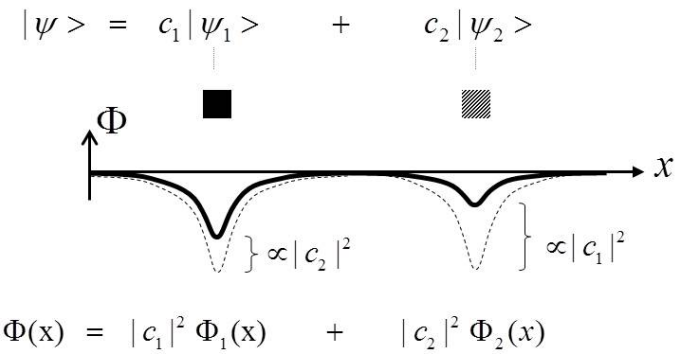

Fig. 4: Gravitational potential of the superposition generated by the single-photon experiment in Figure 2.

where $\Phi_1(\mathbf{x})$ and $\Phi_2(\mathbf{x})$ are the gravitational potentials resulting from the mass distributions $\rho_1(\mathbf{x})$ and $\rho_2(\mathbf{x})$ respectively. The analysis of semiclassical gravity in [1] showed that the sharing of a common gravitational potential leads to energy increases of the states with respect to the case that they must not share the gravitational potential with the other. The energy increases of the states are proportional to the intensity $|c_i|^2$ of the respective competing state, and scale with the Diósi-Penrose energy E_{G12} as follows [1]:

$$\begin{matrix} E_{G1} = |c_2|^2 E_{G12} \\ E_{G2} = |c_1|^2 E_{G12} \end{matrix} \quad . \qquad \textit{energy increases of states} \qquad (6)$$

This result can be confirmed from Figure 4, illustrating the mean gravitational potential of the superposition generated by the single-photon experiment in Figure 2. The gravitational potential of each state increases, where the increase is given by the gap between the mean potential and the state's own gravitational potential. This potential gap, respectively the state's energy increase, is proportional to the intensity $|c_i|^2$ of the competing state (cf. Figure 4) multiplied by the Diósi-Penrose energy E_{G12} (Equation 3), which can be easily recapitulated for a large displacement between the states, where the Diósi-Penrose energy simplifies to $E_{G12}{=}{-}\int d^3\mathbf{x}\rho_1(\mathbf{x})\Phi_1(\mathbf{x}){=}{-}\int d^3\mathbf{x}\rho_2(\mathbf{x})\Phi_2(\mathbf{x})$.

With the help of the states' energy increases E_{Gi}, we can construct so-called *detuning actions* $S_{Gi}(\bar{t})$ for the paths by integrating the energy increase E_{Gi} from the beginning of the path at t_s until the spacetime border at $\bar{t}$ as follows [1]:

$$\begin{matrix} S_{G1}(\bar{t}) = \int_{t_s}^{\bar{t}} dt E_{G1}(t) \\ S_{G2}(\bar{t}) = \int_{t_s}^{\bar{t}} dt E_{G2}(t) \end{matrix} \quad . \qquad \textit{detuning actions} \qquad (7)$$

The paths' detuning actions $S_{Gi}(\bar{t})$, whose physical meaning will become obvious later, can be expressed by the competition action $S_{G12}(\bar{t})$ between the paths as follows:

$$\begin{matrix} S_{G1}(\bar{t}) = |c_2|^2 S_{G12}(\bar{t}) \\ S_{G2}(\bar{t}) = |c_1|^2 S_{G12}(\bar{t}) \end{matrix} \quad . \qquad (8)$$

Similar to the energy increases, the detuning actions of the paths are proportional to the intensity $|c_i|^2$ of the competing path. This means that the paths detune each other. This mutual detuning of the paths plays an important role in the collapse mechanism explained in the next step.

Step 2: Reduction point in time

To explain how and when the wavefunction's evolution becomes unstable for reconfiguration, we assume a small fluctuation of spacetime geometry in favour of one of the states. Since the metric field can be expressed by the gravitational potential in the Newtonian limit, we regard a small fluctuation Δ of the gravitational potential in favour of State 2 as

$$\Phi = (|c_1|^2 - \Delta)\Phi_1 + (|c_2|^2 + \Delta)\Phi_2 \quad . \tag{9}$$

This leads to an increase of Path 1's and to a decrease of Path 2's detuning action as follows:

$$\begin{aligned} dS_{G1} &= +\Delta \cdot S_{G12}(\bar{t}) \\ dS_{G2} &= -\Delta \cdot S_{G12}(\bar{t}) \end{aligned} \quad . \tag{10}$$

Now we come to the key of the collapse mechanism: the question of how the wavepacket's evolution reacts to a change of a path's detuning action. For this, we must take into account that the wavefunction's evolution is not only governed by the unitary evolution, but must also satisfy some boundary condition on the spacetime border. Due to this boundary condition, the evolution of the wavepackets does, to some extent, resemble standing waves on the interval $[t_s, \bar{t}\,]$. An increase of Path 1's detuning action dS_{G1} increases the frequency of its wavepacket, since the gravitational potential on the path increases by $\Delta|\Phi_1|$. Due to the boundary condition on the spacetime border, the frequency of the wavepacket can only increase in discrete steps. Therefore, the frequency increase must be spread over the allowed discrete frequencies, which leads to a spectral broadening of the wavepacket. This in turn leads to an intensity drop of the wavepacket due to the divergence of phases of its partial waves. The intensity drop of a wavepacket $-d|c_i|^2$, which must always have along the path the same amount due to the norm conservation of unitary evolution, depends on the increase of the path's detuning action dS_{Gi} as follows:

$$\frac{d|c_i|^2}{|c_i|^2} = -\frac{dS_{Gi}}{\hbar} \; . \tag{11}$$

This intuitively expected result is derived in the appendix.

The increase of Path 1's detuning action (Equation 10) leads with Equation (11) to an intensity drop of this path of $d|c_1|^2 = -|c_1|^2 \Delta \cdot S_{G12}(\bar{t})/\hbar$. The norm conservation of unitary

evolution enforces that, due to the intensity drop of Path 1, more intensity is rerouted to Path 2 at the splitting point of the wavepackets. Hence, the intensity of Path 2 increases by $d|c_2|^2{=}|c_1|^2\Delta \cdot S_{G12}(\bar{t})/\hbar$. Accordingly, the decrease of Path 2's detuning action leads to an increase of its intensity of $d|c_2|^2{=}|c_2|^2\Delta \cdot S_{G12}(\bar{t})/\hbar$ and enforces that less intensity is rerouted to Path 1 at the splitting point. Both effects together lead with $|c_1|^2+|c_2|^2 = 1$ to

$$d|c_2|^2 = -d|c_1|^2 = \Delta \cdot \frac{S_{G12}}{\hbar} \quad . \tag{12}$$

This result shows that the fluctuation Δ of the gravitational potential (respectively spacetime geometry) in favour of State 2 (Equation 9) leads, via the increase of Path 1's and the decrease of Path 2's detuning action, to an intensity shift to State 2, which has exactly the right amount to induce this fluctuation Δ when the competition action between the paths $S_{G12}(\bar{t})$ coincides with Planck's quantum of action $\hbar$. Consequently, the wavefunction's evolution can only reconfigure when the spacetime border has reached the position $\bar{t}_C$, at which the competition action between the paths coincides with Planck's quantum of action, which is our reduction condition according to Equation (1). How the wavefunction's evolution reconfigures at this critical position of the spacetime border will be explained in the next step.

Step 3: Quasi-abrupt reconfiguration of wavefunction's evolution

For the discussion of how the wavefunction's evolution reconfigures at the reduction position $\bar{t}_C$ of the spacetime border, we assume a small intensity fluctuation in favour of State 2. This intensity fluctuation changes the gravitational potential (respectively spacetime geometry) slightly in favour of this state (cf. Equation 5). According to the discussion above, this change of the gravitational potential in favour of State 2 leads to more intensity being routed to Path 2 at the splitting point, which amplifies the initial fluctuation. This in turn leads to an even larger change of the gravitational potential in favour of State 2, which increases the routing of intensity to Path 2 further. Thus, we enter a self-reinforcing loop, which does not stop until the intensity of State 1 has completely vanished. In the same way, an intensity fluctuation in favour of State 1 leads to a complete vanishing of Path 2. The vanishing of one of the paths, as illustrated in Figure 3, is physically caused via the divergence of phases of the paths' partial waves, i.e. by destructive interference.

Since the wavefunction's evolution becomes unstable for reconfiguration only at exactly the critical position $\bar{t}_C$ of the spacetime border, and since it reconfigures by a self-reinforcing mechanism, the collapse of the wavefunction can be regarded as quasi-abrupt. In a more refined model, collapse is expected to happen in a small interval $\Delta\bar{t}$ around the critical position $\bar{t}_C$.

4 Classical scenarios

In this section, we introduce an important concept for the formulation of the Dynamical Spacetime approach, the so-called *classical scenarios*, which we already used for the analysis of semiclassical gravity in Part 1 [1]. In this concept, the state vector's evolution is decomposed into a superposition of evolutions resembling approximately classical trajectories of the system; the classical scenarios. This decomposition can be performed independently of the chosen Lorentz frame. In relativistic quantum mechanics, the state vector's evolution can be followed up on arbitrarily chosen sequences of spacelike hypersurfaces $\sigma(\tau)$ over the sequence parameter τ with the Tomonaga-Schwinger equation [1, 54, 55], which can be understood as the relativistic equivalent of Schrödinger's equation. We define a decomposition of the state vector's evolution $|\psi(\tau)>\equiv|\psi(\sigma(\tau))>$ into classical scenarios $|\tilde{\psi}_i(\tau)>$ as follows:

$$|\psi(\tau)>=\sum_i c_i|\tilde{\psi}_i(\tau)> \quad , \tag{13}$$

with $<\tilde{\psi}_i(\tau)|\tilde{\psi}_i(\tau)>=1$ and $\sum_i |c_i|^2=1$. The upper right part of Figure 5 shows the state vector's evolution in configuration space for the three-detector experiment in the upper left of the figure, where the state vector's evolution is followed up on an arbitrarily chosen hypersurface sequence $\sigma(\tau)$ with the Tomonaga-Schwinger equation over the sequence parameter τ. The lower part of the figure shows the evolutions of the three classical scenarios $|\tilde{\psi}_1(\tau)>$, $|\tilde{\psi}_2(\tau)>$ and $|\tilde{\psi}_3(\tau)>$ in configuration space and the corresponding behaviour in spacetime.

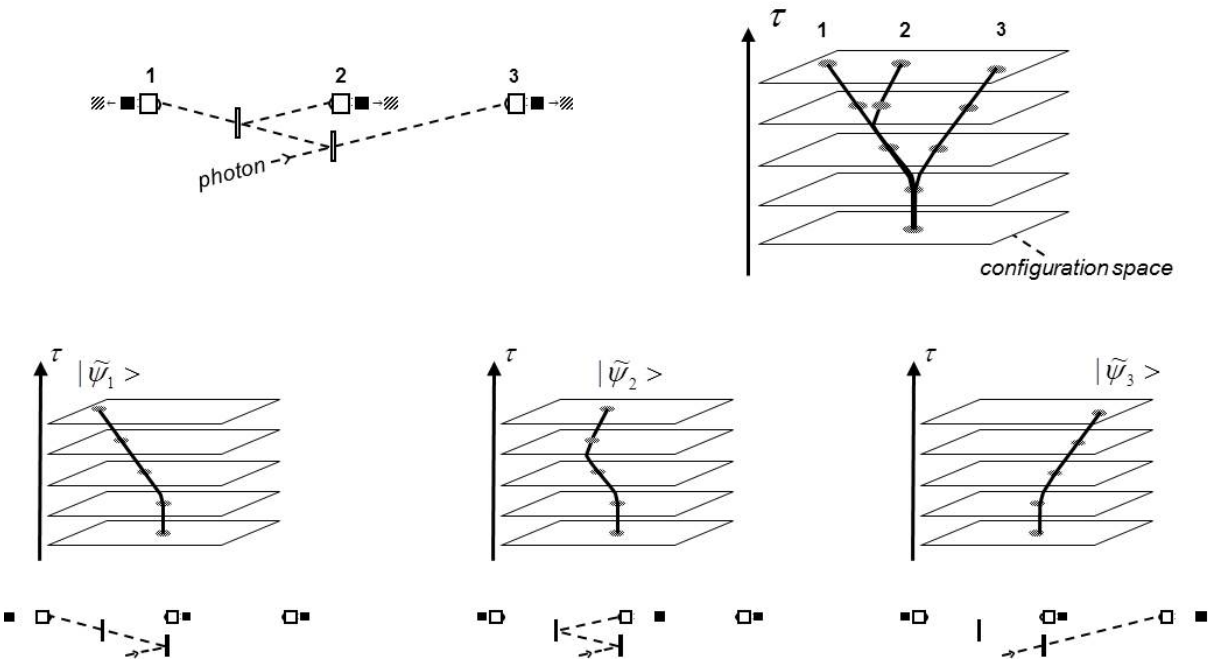

Fig. 5: Three classical scenarios $|\tilde{\psi}_1(\tau)>$, $|\tilde{\psi}_2(\tau)>$ and $|\tilde{\psi}_3(\tau)>$ (middle part) of the three-detector experiment in the upper left, which are defined by following up the state vector's evolution $|\psi(\tau)>$ on classical paths in configuration space (upper right), for which the system evolves on classical trajectories, as shown at the bottom.

The classical scenarios are defined by following up the state vector's evolution on classical paths in configuration space, for which the system evolves on classical trajectories in spacetime. At e.g. the Classical Scenario 1 $|\tilde{\psi}_1(\tau)>$, the photon is completely reflected at the first, and completely transmitted by the second beam splitter, and only detected by Detector 1, as illustrated in the lower left of Figure 5. The classical scenarios are not solutions of the Tomonaga-Schwinger equation at the parameters τ, at which state vector $|\psi(\tau)>$ splits into two wavepackets in configuration space, which is the case when the photon enters a beam splitter. To fulfil the decomposition of the vector's evolution according to Equation (13) at the regions where several classical scenarios refer to the same root wavepacket, their phases must be chosen suitably. At e.g. the common root wavepacket of all classical scenarios, their phases must satisfy $|\sum_i |c_i| e^{i\varphi_i}|=1$. The convention of classical scenarios is independent of the chosen hypersurface sequence $\sigma(\tau)$, and can be regarded as Lorentz invariant.

The as-defined classical scenarios play an important role in the formulation of the Dynamical Spacetime approach, since the quasi-abrupt reconfigurations of the wavefunction's evolution at the critical positions of the spacetime border $\bar{\sigma}(\bar{\tau}_{C})$ can be described by intensity shifts between the classical scenarios. This follows from the norm conservation of unitary evolution. At the collapse event illustrated in Figure 3, the two possible evolutions after reconfiguration are the two classical scenarios of the experiment in Figure 2. At collapse, the intensity of Scenario 1 is shifted either completely to Scenario 2, or vice versa. The intensity shifts between the classical scenarios at collapse must be accompanied by readjustments of their phases φ_{i} at the regions where they refer to common root wave packets to satisfy Equation (13), also after the wavefunction's reconfiguration.

The "classical scenario"-convention allows us to generalise our former definitions of the competition and detuning actions in Section 3. The competition action (Equation 2), which has so far been defined between paths, and begins at t_{s} when the root wavepacket splits, can be defined between classical scenarios as follows:

$$S_{G12}(\bar{t}) \equiv \int_{..}^{\bar{t}} dt E_{G12}(t) \quad . \qquad \textit{competition action (Newtonian limit)} \tag{14}$$

The Diósi-Penrose energy E_{G12} is now integrated over the entire evolution of the classical scenario: not from the splitting point t_{s}. The detuning actions, which were also defined for paths (Equation 7), can be generalised for classical scenarios in the same way:

$$\begin{aligned} S_{G1}(\bar{t}) &= \int_{..}^{\bar{t}} dt E_{G1}(t) \\ S_{G2}(\bar{t}) &= \int_{..}^{\bar{t}} dt E_{G2}(t) \end{aligned} \quad . \qquad \textit{detuning actions (Newtonian limit)} \tag{15}$$

5 Relativistic generalisation

In this section, we generalise our derivation of the collapse mechanism in Section 3, which has been performed so far for the Newtonian limit and a propagation of the spacetime border in alignment with the experiment's rest frame, for the relativistic case and arbitrary propagations of the spacetime border $\bar{\sigma}(\bar{\tau})$.

In Part 1 [1], it was found that the relativistic generalisation of the competition action between classical scenarios $S_{G12}(\bar{t})$ (Equation 14) follows from the decomposition of the Einstein-Hilbert action [4] of a superposition of classical scenarios ($c_1|\tilde{\psi}_1(\tau)>+c_2|\tilde{\psi}_2(\tau)>$) on the spacetime region until the spacetime border $\bar{\sigma}(\bar{\tau})$ according to classical scenarios as follows:

$$S_{EH}(\bar{\tau}) = |c_1|^2 S_{EH1}(\bar{\tau}) + |c_2|^2 S_{EH2}(\bar{\tau}) + |c_1|^2|c_2|^2 S_{G12}(\bar{\tau}) \ , \tag{16}$$

where $S_{EH1}(\bar{\tau})$ and $S_{EH2}(\bar{\tau})$ are respectively the Einstein-Hilbert actions of Classical Scenarios 1 and 2 alone, and $S_{G12}(\bar{\tau})$ the relativistic generalisation of the competition action between the scenarios. This decomposition refers to weak gravitational fields, for which Einstein's field equations can be linearised. The competition action between the classical scenarios $S_{G12}(\bar{\tau})$ is given by the following covariant expression [1]:

$$S_{G12}(\bar{\tau}) = \frac{1}{2}\int_{..}^{\bar{\sigma}(\bar{\tau})} \frac{d^4x}{c}(T_1(x) - T_2(x))(\sqrt{-g_2(x)} - \sqrt{-g_1(x)}) \ , \tag{17}$$

competition action (relativistic)

where $T_i(x)$ are the contracted energy momentum tensor fields of the classical scenarios ($T_i(x) \equiv T^{\mu}_{\ \mu i}(x)$) and $\sqrt{-g_i(x)}$ the factors of the covariant volume elements following from the metric fields of the classical scenarios $h_{\mu\nu i}(x)$ by $g_i(x) \equiv det(\eta_{\mu\nu} + h_{\mu\nu i}(x))$, where $\eta_{\mu\nu}$ is the Minkowski metric ($\eta_{\mu\nu} \equiv diag(1,-1,-1,-1)$). The classical scenarios' metric fields $h_{\mu\nu i}(x)$ follow from their energy momentum tensor fields $T_{\mu\nu i}(x)$ by solving the linearised Einstein field equations. In the Newtonian limit, Equation (17) passes into our former definition of the competition action according to Equations (14) and (2). The differences of the contracted energy momentum tensor fields $T_1(x) - T_2(x)$ pass into the difference of the mass distributions $\rho_1(\mathbf{x}) - \rho_2(\mathbf{x})$; and the difference of the factors of the covariant volume elements $\sqrt{-g_2(x)} - \sqrt{-g_2(x)}$ into the difference of the gravitational potentials $\Phi_2(\mathbf{x}) - \Phi_1(\mathbf{x})$ (cf. Equation 3). This follows with the approximations

[4] The Einstein-Hilbert action on the spacetime region until the spacetime border $\bar{\sigma}$ is given by

$$S_{EH}(\bar{\tau}) = \int_{...}^{\bar{\sigma}(\bar{\tau})} \frac{d^4x}{c}\sqrt{-g(x)}\left(\frac{R(x)}{2\kappa} + L_M(x)\right)$$

where $d^4x\sqrt{-g(x)}$ is the covariant volume element, $R(x)$ the tension scalar, $L_M(x)$ the Lagrangian density of all matter fields and $\kappa = 8\pi G/c^4$ [53]. The factor $1/c$ in the volume element is introduced to obtain the correct dimension of action (i.e. $energy \cdot time$).

$T(x) \approx c^2 \rho(x)$ and $\sqrt{-g(x)} \approx 1 + \Phi(x)/c^2$ for the Newtonian limit. In Part 1 [1], the competition between classical scenarios was interpreted as a measure of how much the preferred spacetime geometries of the scenarios differ from each other, and of how strong they compete for spacetime geometry. This interpretation intuitively follows from the decomposition of the Einstein-Hilbert action (Equation 16).

The relativistic generalisation of the classical scenarios' detuning actions $S_{Gi}(\bar{\tau})$ (Equation 15) was defined in Part 1 [1] by the increases of their Einstein-Hilbert actions $S_{EHi}(\bar{\tau})$ with respect to the case that they must not share spacetime geometry with the other scenario. These increases yield [1]:

$$\begin{aligned} S_{G1}(\bar{\tau}) &= |c_2|^2 S_{G12}(\bar{\tau}) \\ S_{G2}(\bar{\tau}) &= |c_1|^2 S_{G12}(\bar{\tau}) \end{aligned} \quad . \qquad \textit{detuning actions (relativistic)} \tag{18}$$

This result is identical to the Newtonian limit (Equation 8), where the detuning actions of the classical scenarios are also proportional to the intensity $|c_i|^2$ of the respectively competing scenario, and also scale with the competition action between them. In the Newtonian limit, our relativistic definition of the detuning action (via the increases of the scenarios' Einstein-Hilbert actions) can, according to Equation (15), be calculated by the integral of the states' energy increases $E_{Gi}(t)$ over time, which we will need below.

In the relativistic case, the wavefunction's evolution becomes as in the Newtonian limit unstable for reconfiguration, when the competition action between the classical scenarios $S_{G12}(\bar{\tau})$ reaches Planck's quantum of action (cf. Equation 1):

$$S_{G12}(\bar{\tau}_C) = \hbar \quad . \qquad \textit{reduction condition (relativistic)} \tag{19}$$

For the recapitulation of this result, the reader is referred to the following and more mathematical derivation of the reduction condition in Section 8.1. This derivation is based on the norm conservation of unitary evolution, Equation (18) and Equation (11) describe how the intensity of a classical scenario reacts to changes of its detuning action. To show that Equation (11) is also valid for the relativistic case, where a change of the detuning action dS_{Gi} describes the change of the classical scenario's Einstein-Hilbert action, one has to become aware that the change of the detuning action divided by Planck's quantum of action $dS_{Gi}/\hbar$ describes, according to the derivation of Equation (11) in the appendix, the impact on the quantum mechanical phase $\Delta\varphi$ of the classical scenario. This relation between action and phase is assumed at path integrals for the action of the variation principle. The validity of this relation for the classical scenario's Einstein-Hilbert action can be explicitly shown for the Newtonian limit, where changes of the Einstein-Hilbert action are given by the changes of energy integrated over time, as discussed above.

6 Quantum correlations

In this section, we show how the quantum correlations observed in single-photon and EPR experiments can be explained with help of the so-far derived collapse mechanism.

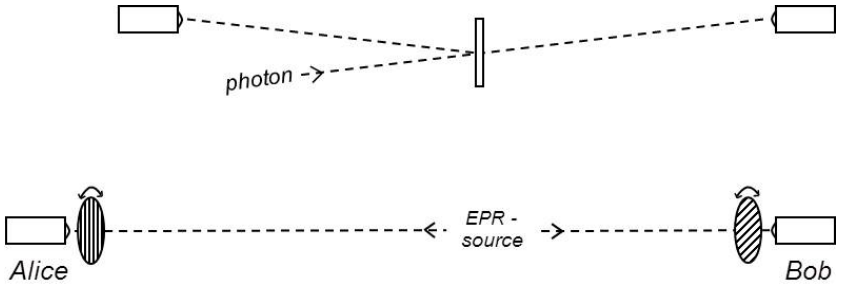

Fig. 6: Single-photon and EPR experiment with free choice of measurements.

Single-photon experiments
The quantum correlations occurring in the single-photon experiment in the upper part of Figure 6, in which either the left or the right detector detects the photon (but never both together), can be explained with the reconfigurations of the wavefunction's evolution in Figure 3, where the photon after collapse is either completely reflected or transmitted by the beam splitter.

EPR experiments
The Dynamical Spacetime approach can also explain the correlations in EPR experiments with the free choice of measurements, as the one in the lower part of Figure 6, in which Bob and Alice can freely choose the orientation of their polarisation filters shortly before the photon's arrival. To simplify discussion, we assume that Alice's arm is chosen to be at least $c\bar{t}_C$ longer than Bob's, which ensures that Bob reduces the superposition by his measurement. Bob can then determine, by choosing of the orientation of his polarisation filter, between which two polarisation states a competition action is built up. When the competition action (caused by Bob's measurement) reaches Planck's quantum of action, the superposition reduces to one of the two polarisation states, which Bob has determined by his choice. Since the abrupt reconfiguration of the wavefunction's evolution covers both Bob's and Alice's locations, the polarisation of Alice's photon instantaneously changes (according to Bob's choice) before it arrives at her detector. Thus, Alice will observe the correlations predicted by quantum theory for any choice of the orientation of her polarisation filter.

This instantaneous transmission of the photon polarisation to Alice according to Bob's choice is a faster-than-light mechanism [5]. This prediction of the Dynamical Spacetime approach does not lead to a conflict with relativity, as we will show in the next section.

[5] Note that the correlations in EPR experiments cannot be used for signalling, as shown by Eberhard in the 1970s [56, 57].

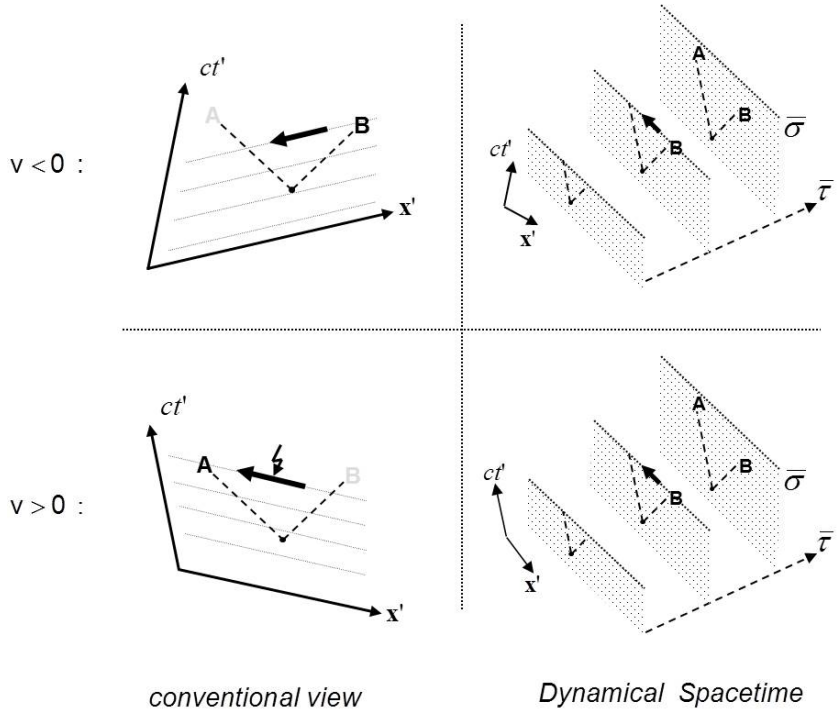

Fig. 7: Illustration of instantaneous transmission of the photon polarisation from Bob to Alice for Lorentz frames with negative and positive velocities, in the conventional view on relativity and in the Dynamical Spacetime approach.

No conflict with relativity

The Dynamical Spacetime approach leads to a new view on relativity. In the conventional view on relativity, in which system's evolution can be followed up along free selectable Lorentz frames, an instantaneous transmission of the photon polarisation from Bob to Alice leads to contradictions, since there are Lorentz frames in which the causality chain is inverted. This is illustrated in the left-hand side of Figure 7, showing an instantaneous transmission from Bob to Alice for Lorentz frames with positive and negative velocities. In the Lorentz frame with positive velocity, Alice receives a signal before Bob has sent it.

In the Dynamical Spacetime approach, causality does not evolve along free selectable Lorentz frames in spacetime. It is rather driven by the expansion of spacetime in the way that the solution of the wavefunction's evolution has to be newly determined for each expansion of spacetime. This means that causality evolves over the dynamical parameter $\bar{\tau}$, quasi-orthogonal to spacetime, as illustrated in the right-hand side of Figure 7. A change of Lorentz frame therefore has no impact on the causality chain, as one can see from the right-hand side of Figure 7, and one obtains no contradiction in the Lorentz frame with positive velocity.

Lorentz invariance

The Dynamical Spacetime approach is Lorentz invariant. The wavefunction's evolution on the spacetime region until the spacetime border can be calculated with the

Tomonaga-Schwinger equation, independently of the chosen Lorentz frame. Furthermore, the competition action $S_{G12}(\bar{\tau})$ following from the decomposition of the Einstein-Hilbert action, which determines the critical position of spacetime border for collapse according to $S_{G12}(\bar{\tau}_C)=\hbar$, is covariant. What remains is that the propagation of the spacetime border $\bar{\sigma}(\bar{\tau})$ distinguishes a Lorentz frame, such as e.g. the experiment's rest frame, as assumed in Section 3. However, if one assumes that the dynamics of spacetime border's propagation $\bar{\sigma}(\bar{\tau})$ is Lorentz invariant, the distinction of a Lorentz frame is not system-immanent, but follows from the initial condition chosen for spacetime border's propagation. We return to how to choose this initial condition in Section 13.

No conflict with the Free Will theorem

The Dynamical Spacetime approach addresses the claim of the Free Will theorem of Conway and Kochen [38, 39] that in special EPR experiments with free choice of measurements (in the sense that the choices are not functions of the past), the information about the choices must travel infinitely fast between the measurement partners, since the Dynamical Spacetime approach explains the quantum correlations by a faster-than-light mechanism.

7 Reduction probabilities

In this section, we come to the second important result of the Dynamical Spacetime approach: its capability to forecast reduction probabilities on the basis of a physical argument. The forecast of reduction probabilities was not made a subject in the established reduction models, such as the dynamical reduction models [28] and Bohmian mechanics [5,6]. They postulate Born's rule instead of deriving it. This has three reasons. First, there are no experimental results, which seriously allows us to doubt the correctness of Born's rule. Secondly, there exists several proofs of Born's rule, deriving it from fundamental principles, such as those of Gleason [58], Deutsch [59], Zurek [60, 61] and others [62, 63]. Thirdly, there is a fear that deviations from Born's rule could lead to faster-than-light signalling and contradict relativity, since some of the proofs of Born's rule are based on the impossibility of faster-than-light signalling [61, 62]. The Dynamical Spacetime approach, explicitly predicting a faster-than-light mechanism, allows for a new view on reduction probabilities and Born's rule.

The question with which probability the wavefunction's evolution reconfigures to a state when wavefunction's evolution becomes unstable for reconfiguration at the reduction point in time $\bar{t}_{C}$ can be related to the question of how frequently the intensities of the states of the superposition fluctuate for decay. This can be expressed in terms of the so-called *decay-trigger rates* of the states. The decay-trigger rates can be derived from the argument that the classical scenarios' detuning actions (Equation 15) are permanently increasing when spacetime border moves on. In the Newtonian limit and when spacetime border's propagation is aligned with the experiment's rest frame, the increase of a scenario's detuning action dS_{Gi} is $dS_{Gi}=E_{Gi}(\bar{t})d\bar{t}$, when spacetime border moves by $d\bar{t}$ (cf. Equation 15). According to Equation (11), this increase of the detuning action would lead to an intensity drop of the path of $d|c_i|^2/|c_i|^2=-E_{Gi}(\bar{t})d\bar{t}/\hbar$. However, since the intensity of a path cannot drop, except at the reduction point in time $\bar{t}_{C}$, we reinterpret this expected intensity drop as the probability $dp_{i\downarrow}$ for a decay-fluctuation, i.e. the probability for a decay-trigger. This leads to the following decay-trigger rates of State 1 and 2 describing the probability for a decay-trigger during spacetime border moves by $d\bar{t}$:

$$\begin{array}{l} \dfrac{dp_{1\downarrow}}{d\bar{t}} = \dfrac{E_{G1}(\bar{t})}{\hbar} \\ \dfrac{dp_{2\downarrow}}{d\bar{t}} = \dfrac{E_{G2}(\bar{t})}{\hbar} \end{array} \quad . \qquad \textit{decay-trigger rates (Newtonian limit)} \qquad (20)$$

The states' decay-trigger rates $dp_{i\downarrow}/d\bar{t}$ are proportional to the states' energy increases E_{Gi} resulting from the sharing of spacetime geometry in semiclassical gravity. This result will play an important role later.

For the relativistic case and arbitrary propagations of the spacetime border $\bar{\sigma}(\bar{\tau})$, we obtain with the approach above the following result:

$$\begin{array}{l} \dfrac{dp_{_{1\downarrow}}}{d\bar{\tau}} = \dfrac{\frac{d}{d\bar{\tau}}S_{_{G1}}(\bar{\tau})}{\hbar} \\ \dfrac{dp_{_{2\downarrow}}}{d\bar{\tau}} = \dfrac{\frac{d}{d\bar{\tau}}S_{_{G2}}(\bar{\tau})}{\hbar} \end{array} \quad . \qquad \textit{decay rates of states (relativistic)} \tag{21}$$

This result has an intuitive physical illustration. The probability for a decay-trigger $dp_{_{i\downarrow}}$ during spacetime border to move from $\bar{\sigma}(\bar{\tau})$ to $\bar{\sigma}(\bar{\tau}+d\bar{\tau})$ is given by the increase of the classical scenario's detuning action $dS_{_{Gi}}$ during this interval divided by Planck's quantum of action $\hbar$.

Since the states' energy increases scale according to Equation (6) with the intensity of the respective competing state ($E_{_{G1}}\propto|c_{_2}|^2$, $E_{_{G2}}\propto|c_{_1}|^2$) in favour of which the state will decay, we obtain with Equation (20) the reduction probabilities $p_{_i}$ proportional to the state's intensity $|c_{_i}|^2$ in accordance with Born's rule:

$$\begin{array}{l} p_{_1} = |c_{_1}|^2 \\ p_{_2} = |c_{_2}|^2 \end{array} \quad . \qquad \textit{Born's rule} \tag{22}$$

The same result follows with Equation (21) for the relativistic case, since the classical scenarios' detuning actions also scale with the intensity of the respective competing scenario ($S_{_{G1}}(\bar{\tau})\propto|c_{_2}|^2$, $S_{_{G2}}(\bar{\tau})\propto|c_{_1}|^2$; cf. Equation 18).

In the Dynamical Spacetime approach, there is a relation between Born's rule and semiclassical gravity. Energy increases, respective decay-trigger rates, being proportional to the intensity of the competing state in favour of which the state will decay, follow from the fact that the states share the mean gravitational potential in semiclassical gravity.

In Section 9, our derivation of Born's rule for two-state superposition will be generalised for typical quantum mechanical experiments.

8 Model for superpositions of more than two states

In this section, we refine our collapse model for superpositions of more than two states. In Section 8.1, we derive the so-called *reconfiguration equation* first for two-state superpositions, whose solutions determine when the wavefunction's evolution becomes unstable for reconfiguration, which confirms the results derived so far. In Section 8.2, we recapitulate the concepts of so-called *local bundles*, *local Diósi-Penrose energies* and *local competition actions*, which were introduced in Part 1 [1] for the analysis of semiclassical gravity, and which are needed for the discussion of superpositions of more than two states. In Section 8.3, we generalise the reconfiguration equation of Section 8.1 for superpositions of more than two states; and in Section 8.4, we derive the so-called *reconfiguration rule* for the calculation of reduction probabilities.

8.1 Reconfiguration equation for two-state superpositions

In this section, we derive the so-called *reconfiguration equation* first for two-state superpositions. The solutions of this equation describe whether the intensities between classical scenarios can be shifted; its solutions allow us to determine the critical positions of the spacetime border $\bar{\tau}_{C}$ at which the wavefunction's evolution becomes unstable for reconfiguration.

For the following derivation, we abbreviate the intensities $|c_{i}|^{2}$ of the classical scenarios $|\tilde{\psi}_{i}(\tau)>$ (cf. Equation 13) as follows:

$$I_{i} \equiv |c_{i}|^{2} \quad . \qquad \textit{intensities of classical scenarios} \tag{23}$$

According to Equation (18), the detuning actions S_{G1} and S_{G2} of the classical scenarios of a two-state superposition can change due to intensity changes dI_{i} of the respectively competing scenario, or due to an increase of the competition action between the scenarios, when the spacetime border moves by $d\bar{\tau}$, as follows:

$$\begin{aligned} dS_{G1} &= S_{G12}(\bar{\tau})dI_{2} + I_{2}\tfrac{d}{d\bar{\tau}}S_{G12}(\bar{\tau})d\bar{\tau} \\ dS_{G2} &= S_{G12}(\bar{\tau})dI_{1} + I_{1}\tfrac{d}{d\bar{\tau}}S_{G12}(\bar{\tau})d\bar{\tau} \end{aligned} \quad . \tag{24}$$

According to Equation (11) and the norm conservation of unitary evolution ($dI_{1}+dI_{2}=0$), a change of Classical Scenario 1's detuning action of dS_{G1} changes its intensity by $dI_{1}/I_{1}=-dS_{G1}/\hbar$ and the intensity of Scenario 2 by $dI_{2}/I_{2}=dS_{G1}/\hbar$. Calculating the impact of a change of Classical Scenario 2's detuning action dS_{G2} accordingly, we obtain

$$\begin{aligned} dI_{1} &= -\frac{dS_{G1}}{\hbar}I_{1} + \frac{dS_{G2}}{\hbar}I_{2} \\ dI_{2} &= \quad \frac{dS_{G1}}{\hbar}I_{1} - \frac{dS_{G2}}{\hbar}I_{2} \end{aligned} \quad . \tag{25}$$

By inserting Equation (24) into Equation (25), we arrive at the reconfiguration equation:

$$\begin{aligned} dI_1 &= \frac{S_{G12}(\bar{\tau})}{\hbar}(I_2 dI_1 - I_1 dI_2) \\ dI_2 &= \frac{S_{G12}(\bar{\tau})}{\hbar}(I_1 dI_2 - I_2 dI_1) \ , \end{aligned} \tag{26}$$

reconfiguration equation (two-state superposition)

in which all terms that depend on the movement of the spacetime border (see terms with $\frac{d}{d\bar{\tau}} S_{G12}(\bar{\tau})$ in Equation 24) have cut off. To determine the solutions to this equation, it is helpful to transform it with $dI_1 + dI_2 = 0$ and $I_1 + I_2 = 1$ to

$$\begin{pmatrix} dI_1 \\ dI_2 \end{pmatrix} = \frac{S_{G12}(\bar{\tau})}{\hbar} \begin{pmatrix} 1 & 0 \\ 0 & 1 \end{pmatrix} \begin{pmatrix} dI_1 \\ dI_2 \end{pmatrix} \quad , \tag{27}$$

which only has solutions different to zero, when our reduction condition $S_{G12}(\bar{\tau}) = \hbar$ (Equation 19) is fulfilled. Then Equation (27) has the solutions $d\vec{I} \equiv (dI_1, dI_2)^T \propto \pm(-1, 1)^T$ describing intensity shifts from Classical Scenario 1 to 2 (or vice versa) and the unphysical (not norm conserving) solutions $d\vec{I} \propto \pm(1, 1)^T$. The latter ones are however not solutions to our real reconfiguration equation (Equation 26), and result from the transformation.

8.2 Local bundles, Diósi-Penrose energies and competition actions

In this section, we recapitulate the so-called concepts of *local bundles*, *local Diósi-Penrose energies* and *local competition actions*, which we introduced in Part 1 [1] for the analysis of semiclassical gravity, and which we need to extend our reconfiguration equation for superpositions of more than two states.

Local bundles of states and classical scenarios

The analysis of typical experiments shows that different states often have identical mass distributions on some areas. In the three-detector experiment in Figure 8, which generates a superposition of three states, where each state corresponds to a photon detection in one of the detectors, States 2 and 3 have on the area of Detector 1 identical mass distributions corresponding to the case that the photon is not detected by this detector. The same applies for States 1 and 3 on the area of Detector 2, etc. This leads us to the following definition of *local bundles*:

> When several states or classical scenarios have identical wavefunctions and prefer identical spacetime geometries on an area A, they are a *local bundle* b_κ^A on A.

Here κ is the *bundle index*, for which we use Greek letters, and which is needed to distinguish several bundles on the same *bundle area* A. Two states or scenarios i and j have identical wavefunctions on A, when the parts of the state vectors referring to A are identical ($|\psi_i>_A=|\psi_j>_A$). This assumes that state vector can be decomposed into a part referring to the bundle area A and a part referring to the area outside of A as $|\psi_i>=\psi_i>_A\otimes|\psi_i>_{\neg A}$. Two classical scenarios prefer identical spacetime geometries on A, when the their metric fields $h_{\mu\nu i}(x)$ resulting from the energy momentum tensor fields $T_{\mu\nu i}(x)$ (by solving the linearised Einstein field equations) are identical on A. In the Newtonian limit, two states prefer identical spacetime geometries, when their gravitational potentials $\Phi_i(\mathbf{x})$ resulting from their mass distributions $\rho_i(\mathbf{x})$ are identical, since the metric field can be expressed by the gravitational potential in this limit ($g_{00}\approx 1+2\Phi/c^2$ [53]). The intensity of a local bundle κ is given by the sum over the intensities of its states or classical scenarios as

$$I_\kappa \equiv \sum_{i\in b_\kappa^A} I_i \quad . \qquad \textit{intensities of local bundles} \tag{28}$$

For the three-detector experiment in Figure 8, we can find three bundle areas corresponding to the areas of the three detectors. On the area of Detector 1, we have the local bundle $b_1^{D1}=\{1\}$ consisting of State 1 only, and the local bundle $b_2^{D1}=\{2,3\}$ consisting of States 2 and 3, where b_1^{D1} corresponds to a photon detection, and b_2^{D1} to no photon detection. On the areas of Detectors 2 and 3, we obtain two local bundles accordingly, as shown in the figure.

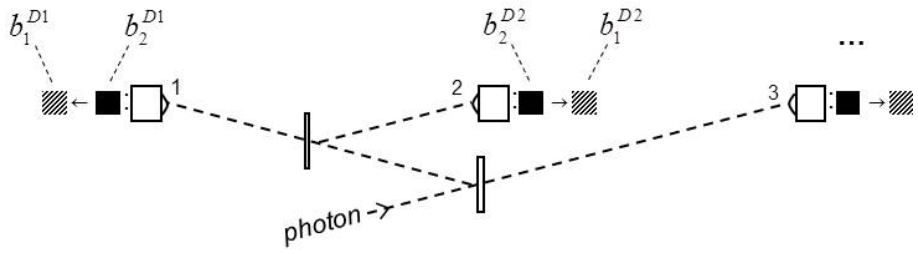

Fig. 8: Single-photon experiment generating a superposition of three states.

Local Diósi-Penrose energies and competition actions

Between two local bundles b_κ^A and b_ν^A on the same bundle area A, we define a so-called local Diósi-Penrose energy by restricting integration to the bundle area A as follows (cf. Equation 3):

$$E_{G\kappa\nu}^A = \frac{1}{2}\int_{\mathbf{x}\in A} d^3\mathbf{x}(\rho_\kappa(\mathbf{x})-\rho_\nu(\mathbf{x}))(\Phi_\nu(\mathbf{x})-\Phi_\kappa(\mathbf{x})) \quad , \quad \textit{local Diósi-Penrose energy} \tag{29}$$

where $\rho_\kappa(\mathbf{x})$, $\rho_\nu(\mathbf{x})$ are the mass distributions, and $\Phi_\kappa(\mathbf{x})$, $\Phi_\nu(\mathbf{x})$ the gravitational potentials of bundle κ and ν respectively. Accordingly, we define the local competition action between two local bundles of classical scenarios as (cf. Equation 17):

$$S^{A}_{G\kappa\nu}(\bar{\tau}) = \frac{1}{2}\int_{\substack{\cdot\cdot \\ x\in A}}^{\bar{\sigma}(\bar{\tau})} \frac{d^4x}{c}(T_{\kappa}(x) - T_{\nu}(x))(\sqrt{-g_{\nu}(x)} - \sqrt{-g_{\kappa}(x)}) \ , \qquad (30)$$

local competition action (relativistic)

where the bundles' contracted energy momentum tensor fields $T_{\kappa}(x)$ and the factors $\sqrt{-g_{\kappa}(x)}$ result from their energy momentum tensor fields $T_{\mu\nu\kappa}(x)$ and metric fields $h_{\mu\nu\kappa}(x)$ by $T_{\kappa}(x)=T^{\mu}{}_{\mu\kappa}(x)$ and $g_{\kappa}(x)=det(\eta_{\mu\nu}+h_{\mu\nu\kappa}(x))$. In the Newtonian limit, the local competition action can be calculated with the local Diósi-Penrose energy similar to Equation (14) as [1]

$$S^{A}_{G\kappa\nu}(\bar{t}) = \int_{\cdot\cdot}^{\bar{t}} dt E^{A}_{G\kappa\nu}(t) \ . \qquad \textit{local competition action (Newtonian limit)} \qquad (31)$$

The local competition between bundles of classical scenarios on the same bundle area A define a measure of how much the preferred spacetime geometries of the classical scenarios differ from each other, and of how strong they compete for spacetime geometry on A.

Energy increases and detuning actions of local bundles

In Part 1 [1], we calculated the energy increases of local bundles of states, which result from sharing the mean gravitational potential with the other bundles on the bundle area A. This calculation yields

$$E^{A}_{G\kappa} = \sum_{\nu\neq\kappa} I_{\nu} E^{A}_{G\kappa\nu} \ . \qquad \textit{energy increases of local bundles} \qquad (32)$$

This result is the intuitively expected generalisation of Equation (6) for the states' energy increases. The energy increase of a local bundle κ on A depends on the intensities I_{ν} of the competing bundles ν on A multiplied by the local Diósi-Penrose energy $E^{A}_{G\kappa\nu}$ between κ and ν.

In the same way, we calculated in Part 1 [1] detuning actions for local bundles of classical scenarios, which yielded

$$S^{A}_{G\kappa}(\bar{\tau}) = \sum_{\nu\neq\kappa} I_{\nu} S^{A}_{G\kappa\nu}(\bar{\tau}) \ . \qquad \textit{detuning actions of local bundles} \qquad (33)$$

This result is the intuitively expected generalisation of Equation (18) for the classical scenarios' detuning actions. The detuning action of a local bundle κ on A depends on the intensities I_{ν} of the competing bundles ν on A multiplied by the local competition $S^{A}_{G\kappa\nu}(\bar{\tau})$ between κ and ν.

Decay-trigger rates of local bundles
Our derivation of the states' decay trigger rates (Equation 20) in Section 7 can be adapted to local bundles. In the Newtonian limit and when the spacetime border's propagation is aligned with the experiment's rest frame, the increase of a local bundle's detuning action $dS^{A}_{G\kappa}$, when the spacetime border moves by $d\bar{t}$, is given by $dS^{A}_{G\kappa}{=}E^{A}_{G\kappa}(\bar{t})d\bar{t}$ (cf. Equation 31), which leads to an intensity drop of the local bundle of $dI_{\kappa}/I_{\kappa}{=}-E^{A}_{G\kappa}(\bar{t})d\bar{t}/\hbar$, which we interpret as the probability $dp^{A}_{\kappa\downarrow}$ for a decay-trigger of the local bundle κ. This leads to the following decay-trigger rates of local bundles:

$$\frac{dp^{A}_{\kappa\downarrow}}{d\bar{t}} = \frac{E^{A}_{G\kappa}}{\hbar} \quad . \qquad \textit{decay-trigger rates of local bundles (Newtonian limit)} \tag{34}$$

The local bundles' decay-trigger rates $dp^{A}_{\kappa\downarrow}/d\bar{t}$ are proportional to their energy increases $E^{A}_{G\kappa}$. The energy increase, respectively decay-trigger rate, of a local bundle κ depends, according to Equation (32), only on the intensities I_{ν} of the bundles ν competing with the bundle on A, and not on the bundle's own intensity I_{κ}. This result will later play an important role.

For the relativistic case and arbitrary propagations of the spacetime border $\bar{\sigma}(\bar{\tau})$, we obatin with our approach the following decay-trigger rates of local bundles:

$$\frac{dp^{A}_{\kappa\downarrow}}{d\bar{\tau}} = \frac{\frac{d}{d\bar{\tau}}S^{A}_{G\kappa}(\bar{\tau})}{\hbar} \quad , \qquad \textit{decay-trigger rates of local bundles (relativistic)} \tag{35}$$

which is the generalisation of Equation (21). This result has as Equation (21) the physical illustration that the probability $dp^{A}_{\kappa\downarrow}$ for a decay-trigger of the local bundle κ on A during the spacetime border moving from $\bar{\sigma}(\bar{\tau})$ to $\bar{\sigma}(\bar{\tau}{+}d\bar{\tau})$ is given by the increase of the bundle's detuning action $dS^{A}_{G\kappa}$ during this interval divided by $\hbar$.

8.3 Reconfiguration equation for superpositions of more than two states

In this section, we extend the reconfiguration equation derived in Section 8.1 for superpositions of more than two states with the help of the concepts of local bundles and competition actions.

With the following derivation of the reconfiguration equation, we assume that our concept of local bundles can be applied. This means that the competition of the classical scenarios for spacetime geometry can be characterised by local competition actions $S^{A}_{G\kappa\nu}(\bar{\tau})$ on some bundle areas A, as in the experiment in Figure 8, for which we identified three bundle areas corresponding to the locations of the three detectors. When we first assume that the photon in the experiment in Figure 8 is absorbed by the left beam splitter and not detected by Detectors 1 and 2 at all, we obtain a two-state superposition, in which only the two local bundles at Detector 3 ($b^{D3}_{1}{=}\{3\}$, $b^{D3}_{2}{=}\{1,2\}$)

compete for spacetime geometry, which is described by the local competition action $S^{D3}_{G\{1,2\}3}$. The reconfiguration equation of this two-state superposition is given by the following two equations on the left (cf. Equation 26):

$$\begin{aligned} dI_3 &= \frac{S^{D3}_{G\{1,2\}3}}{\hbar}(I_{\{1,2\}}dI_3 - I_3 dI_{\{1,2\}}) \\ dI_{\{1,2\}} &= \frac{S^{D3}_{G\{1,2\}3}}{\hbar}(I_3 dI_{\{1,2\}} - I_{\{1,2\}}dI_3) \Rightarrow \begin{cases} dI_1 = \frac{dI_1}{dI_{\{1,2\}}}\frac{S^{D3}_{G\{1,2\}3}}{\hbar}(I_3 dI_{\{1,2\}} - I_{\{1,2\}}dI_3) \\ dI_2 = \frac{dI_2}{dI_{\{1,2\}}}\frac{S^{D3}_{G\{1,2\}3}}{\hbar}(I_3 dI_{\{1,2\}} - I_{\{1,2\}}dI_3) \end{cases} . \end{aligned} \tag{36}$$

The lower equation here can be split into two equations for the two classical scenarios of the bundle $b^{D3}_2{=}\{1,2\}$, as shown on the right, where the intensity shifts of the classical scenarios dI_1 and dI_2 must in addition satisfy $dI_1{+}dI_2{=}dI_{\{1,2\}}$. For the transformed equation system, one is free of how to distribute an intensity change of the bundle $dI_{\{1,2\}}$ on the two classical scenarios, which means that an intensity shift between Classical Scenarios 1 and 2 should not change the physical result. This follows from our bundle definition that the classical scenarios of a bundle must have identical wavefunctions and prefer identical spacetime geometries on the bundle area, which means that an intensity shift between Classical Scenarios 1 and 2 does not change the physical situation on the bundle area of Detector 3. Also applying the procedure above for Detectors 1 and 2, we obtain the following equation for the intensity change of Classical Scenario 1:

$$\begin{aligned} dI_1 = \frac{dI_1}{dI_{\{1,2\}}}\frac{S^{D3}_{G\{1,2\}3}}{\hbar}(I_3 dI_{\{1,2\}} - I_{\{1,2\}}dI_3) + \frac{dI_1}{dI_{\{1,3\}}}\frac{S^{D2}_{G\{1,3\}2}}{\hbar}(I_2 dI_{\{1,3\}} - I_{\{1,3\}}dI_2) \\ + \frac{S^{D1}_{G1\{2,3\}}}{\hbar}(I_{\{2,3\}}dI_1 - I_1 dI_{\{2,3\}}) \end{aligned} . \tag{37}$$

The equations for the intensity changes of Classical Scenarios 2 and 3 can be derived accordingly. Equation (37) can be generalised for any number of bundle areas and for more than two competing bundles on the same bundle area, which leads to the following equation system:

$$dI_i = \sum_{A;\,\kappa \supseteq i} \frac{dI_i}{dI_\kappa} \sum_{\nu \neq \kappa} \frac{S^A_{G\kappa\nu}(\bar{\tau})}{\hbar}(I_\nu dI_\kappa - I_\kappa dI_\nu) \quad , \qquad \textit{reconfiguration equation} \tag{38}$$

in which every equation refers to a state i. In this result, the outer sum runs over all bundle areas A. The condition $\kappa{\supseteq}i$ selects for every bundle area A the bundle κ, which contains the regarded state i. The inner sum runs over all bundles ν, which compete with κ on A.

The critical position of the spacetime border $\bar{\tau}_C$, at which the wavefunction's evolution becomes unstable for reconfiguration, follows from our reconfiguration equation by determining the smallest dynamical parameter $\bar{\tau}$ for which the reconfiguration equation

has solutions $d\vec{I}\equiv(dI_1, dI_2, ..)^T$ different to zero. We call these solutions the *reconfiguration solutions* $d\vec{I}_C$. The reconfiguration solutions $d\vec{I}_C$ can span one or higher dimensional space, as we will see in later discussion.

8.4 Reconfiguration rule

In this section, we derive the so-called *reconfiguration rule*, with which we can calculate how and with which probabilities the wavefunction's evolution reconfigures at the critical positions of the spacetime border $\bar{\tau}_C$.

The reconfiguration equation (Equation 38) has the following important property, with the help of which we can derive how the wavefunction's evolution reconfigures at $\bar{\tau}_C$. When $d\vec{I}_C$ is a solution of the reconfiguration equation for a given intensity vector of classical scenarios $\vec{I}\equiv(I_1, I_2, ..)^T$, it is also a solution for the by $d\vec{I}_C$ shifted intensity vector $\vec{I}+\alpha d\vec{I}_C$, where α is a real number. This property can be easily recapitulated by inserting $\vec{I}+\alpha d\vec{I}_C$ into Equation (38). This means that when the intensity vector of classical scenarios $\vec{I}$ fluctuates in the direction of the reduction solution like $\vec{I}'=\vec{I}+\epsilon d\vec{I}_C$, it can reconfigure without hindrance on the line $\vec{I}'=\vec{I}+\alpha d\vec{I}_C$. This reconfiguration will happen by the self-reinforcing reconfiguration mechanism (described in Section 3) quasi-abruptly, where the reconfiguration does not stop until one component of the intensity vector $\vec{I}'$ has become zero. This means that the intensity vector $\vec{I}'$ after reconfiguration is given by $\vec{I}'=\vec{I}+\hat{\alpha}d\vec{I}_C$, where $\hat{\alpha}$ is the largest positive number for which $\vec{I}+\hat{\alpha}d\vec{I}_C$ has no negative components.

For the following derivation of the reconfiguration rule, we assume that the reduction solutions $d\vec{I}_C$ span a one-dimensional space at $\bar{\tau}_C$. The way in which to treat a higher-dimensional solution space is shown in Section 9 for a concrete example. For a one-dimensional solution space, the intensity vector $\vec{I}$ can reconfigure either to $\vec{I}'_+=\vec{I}+\hat{\alpha}_+ d\vec{I}_C$ or to $\vec{I}'_-=\vec{I}-\hat{\alpha}_- d\vec{I}_C$, where $\hat{\alpha}_+$ and $\hat{\alpha}_-$ are the largest numbers for which $\vec{I}+\hat{\alpha}_+ d\vec{I}_C$ respectively $\vec{I}-\hat{\alpha}_- d\vec{I}_C$ have no negative components. The probabilities of these two reconfigurations depend on which direction ($+d\vec{I}_C$ or $-d\vec{I}_C$) the decay triggers of the local bundles trigger the intensity vector $\vec{I}$. These directions can be determined with the help of the projections of the bundles b^A_κ on the reduction solution $d\vec{I}_C$, which we define by [6]

$$dI^A_{C\kappa} \equiv \sum_i \delta_{i\in b^A_\kappa} dI_{Ci} \quad . \qquad \textit{projection of local bundle } b^A_\kappa \textit{ on } d\vec{I}_C \tag{39}$$

For a negative projection ($dI^A_{C\kappa}<0$), a decay-trigger of bundle b^A_κ triggers the intensity vector $\vec{I}$ in the $+d\vec{I}_C$-direction; and for a positive projection ($dI^A_{C\kappa}>0$) in the $-d\vec{I}_C$-direction. The probabilities p_+ and p_- for the two reconfigurations to $\vec{I}'_+=\vec{I}+\hat{\alpha}_+ d\vec{I}_C$

[6] $\delta_{i\in b^A_\kappa}\equiv 1$ for $i\in b^A_\kappa$, $\delta_{i\in b^A_\kappa}\equiv 0$ for $i\notin b^A_\kappa$.

and $\vec{I}'_{-}=\vec{I}-\hat{\alpha}_{-}d\vec{I}_{C}$ are proportional to the sum of all decay-trigger rates of the bundles $dp^{A}_{\kappa\downarrow}/d\bar{\tau}$ with negative respectively positive projections. This leads to the following reconfiguration rule [7]:

$$\vec{I}\rightarrow\begin{cases}\vec{I}'_{+}=\vec{I}+\hat{\alpha}_{+}d\vec{I}_{C} \quad \textit{with} \quad p_{+}\propto\sum_{A,\kappa}\Theta_{0}(-dI^{A}_{C\kappa})\dfrac{dp^{A}_{\kappa\downarrow}}{d\bar{\tau}}\\ \\ \vec{I}'_{-}=\vec{I}-\hat{\alpha}_{-}d\vec{I}_{C} \quad \textit{with} \quad p_{-}\propto\sum_{A,\kappa}\Theta_{0}(dI^{A}_{C\kappa})\dfrac{dp^{A}_{\kappa\downarrow}}{d\bar{\tau}}\end{cases} \quad , \qquad \textit{reconfiguration rule} \qquad (40)$$

which describes the possible reconfigurations of the intensity vector and the relative probabilities of these reconfigurations. The absolute reconfiguration probabilities follow by normalisation ($p_{+}+p_{-}=1$).

The reconfiguration rule (Equation 40) displays an important property of the Dynamical Spacetime approach. The reconfiguration probabilities p_{+}, p_{-} depend only on the decay-trigger rates $dp^{A}_{\kappa\downarrow}/d\bar{\tau}$ of the local bundles, and not on their intensity vectors $\vec{I}^{A}_{\kappa}$, which we define by

$$I^{A}_{\kappa i}\equiv\delta_{i\in b^{A}_{\kappa}}I_{i} \quad , \qquad \textit{intensity vector } \vec{I}^{A}_{\kappa} \textit{ of local bundle } b^{A}_{\kappa} \qquad (41)$$

and which we will use in the next section. The bundles' decay-trigger rates $dp^{A}_{\kappa\downarrow}/d\bar{\tau}$, which depend, according to Equations (35) and (33), only on the intensities I_{ν} of the competing bundles on A and not on their own intensities I_{κ}, determine how frequently the bundles fluctuate for decay. The intensity vectors of the bundles $\vec{I}^{A}_{\kappa}$ determine the amplitudes of these decay fluctuations. Since the reconfiguration of the wavefunction's evolutions occurs in the Dynamical Spacetime approach by a self-reinforcing reconfiguration mechanism, the amplitudes of the decay fluctuations initiating the reconfigurations play no role for the reduction probabilities. We return to this property of the Dynamical Spacetime approach in Section 10.

[7] $\Theta_{0}(x)=0$ for $x\leq 0$, $\Theta_{0}(x)=1$ for $x>0$.

9 Typical quantum mechanical experiments

In this section, we apply our collapse model to typical mechanical experiments. We will show how our derivation of Born's rule for two-state superpositions in Section 7 can be adapted to these experiments with the help of a property that these experiments have in common. They lead to never more than two local bundles, i.e. to two different mass distributions, at one location, which e.g. refer to the cases that a particle "is", or "is not", detected at the location.

Never more than two local bundles in typical quantum mechanical experiments
Typical quantum mechanical experiments can be categorised in two groups. Experiments with active measuring devices, such as the three-detector experiment in Figure 8; and experiments with passive measuring devices, as e.g. films or cloud chambers. Both groups can be discussed in a common picture by modelling passive measuring devices with a large number of small mass displacing detectors, as shown in Figure 9 for a photon measurement with a film. If one analyses these experiments from the local bundles' point of view, one finds that they exhibit never more than two local bundles on the same bundle area, which refer to the cases that the particle "is", or respectively "is not", detected by the detector on the bundle area, as one can see in Figures 8 and 9. This means that these experiments lead to never more than two different mass distributions at one location.

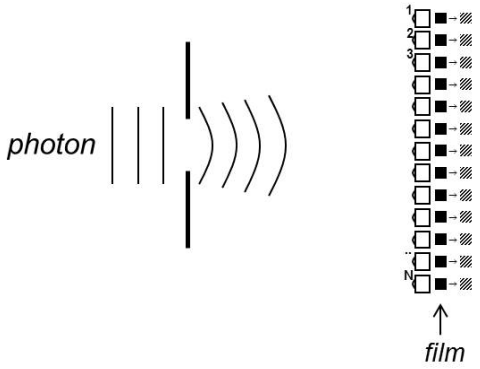

Fig. 9: Measurement of a photon with a film, which can be modelled with a large number of small mass displacing detectors.

Reconfiguration equation and reduction condition
The two local bundles on the bundle area of a detector i in the single photon experiments in Figures 8 and 9 are given as follows. The bundle b_i^{Di} displaying the case that the photon is detected by detector i consists of only state i; and the bundle $b_{\neg i}^{Di}$ displaying the case that the photon is not detected by detector i consists of a superposition of all states except i, which we abbreviate by $\neg i$. The intensity of bundle $b_{\neg i}^{Di}$ is given by $I_{\neg i}{=}\sum_{j\neq i} I_j$. With the relations $I_i{+}I_{\neg i}{=}1$ and $dI_i{+}dI_{\neg i}{=}0$ following from the

norm conservation of unitary evolution, the reconfiguration equation (Equation 38) can be transformed to

$$dI_{_i} = (\sum_i \frac{S_G^{Di}(\bar{\tau})}{\hbar}) dI_{_i} \ , \tag{42}$$

where we abbreviated the local competition actions $S_{Gi\neg i}^{Di}(\bar{\tau})$ between the bundles by $S_G^{Di}(\bar{\tau})$. This equation allows for intensity shifts $d\vec{I}$ only, when the following reduction condition is satisfied:

$$\sum_i S_G^{Di}(\bar{\tau}_{_C}) = \hbar \ , \qquad \textit{reduction condition} \tag{43}$$

which can be regarded as the generalisation of our reduction condition $S_{G12}(\bar{\tau}_{_C})=\hbar$ (Equation 19).

Reconfiguration rule

The energy increases of the local bundles b_i^{Di} and $b_{\neg i}^{Di}$ due to the sharing of spacetime geometry with the other bundle on the bundle area of detector i are given according to Equation (32) by $I_{_{\neg i}} E_G^{Di}$ and $I_{_i} E_G^{Di}$ (with $E_G^{Di} \equiv E_{i\neg i}^{Di}$), which means that the bundles' decay-trigger rates (Equation 34) are proportional to the intensity of the competing bundle. The transformed reconfiguration equation (Equation 42) allows for arbitrary changes of the intensity vector $d\vec{I}$ [8]. Due to this freedom, we can assume that the ratios between the intensities of a bundle's states remain constant when the bundle is triggered for decay. In the same way, we can assume that the ratios between the intensities of the states outside the bundle, whose intensities must increase at the bundle's decay, also remain constant. From this, it follows that a decay of bundle b_i^{Di} leads to a reconfiguration to bundle $b_{\neg i}^{Di}$, and that a decay of bundle $b_{\neg i}^{Di}$ to a reconfiguration to bundle b_i^{Di}. This leads to the following reconfiguration rule [9]:

$$\vec{I} \rightarrow \begin{cases} \frac{1}{I_i} \vec{I}_i^{Di} & \textit{with} \ \ p_{_i} \propto I_{_i} E_G^{Di} \\ \frac{1}{I_{\neg i}} \vec{I}_{\neg i}^{Di} & \textit{with} \ \ p_{_{\neg i}} \propto I_{_{\neg i}} E_G^{Di} \end{cases} , \qquad \textit{reconfiguration rule} \tag{44}$$

which describes $2N$ possible reconfigurations (N = number of detectors). $\frac{1}{I_i}\vec{I}_i^{Di}$ and $\frac{1}{I_{\neg i}}\vec{I}_{\neg i}^{Di}$ are the intensity vectors of bundle b_i^{Di} and $b_{\neg i}^{Di}$, where the factors $\frac{1}{I_i}$ and $\frac{1}{I_{\neg i}}$ are introduced for normalisation. Equation (44) displays what is expected by Born's rule: the reduction probability to a bundle is proportional to its intensity.

The three-detector experiment in Figure 8 reduces when the sum of the three detectors' local competition actions reaches Planck's quantum of action: $S_G^{D1}(\bar{t}_{_C}) + S_G^{D2}(\bar{t}_{_C}) + S_G^{D3}(\bar{t}_{_C}) = \hbar$. Here, the wavefunction's evolution can reconfigure in six different ways. The competition for spacetime geometry between State 1 and Bundle ¬1 on the location of

[8] Equation (42) also allows, like the transformed reconfiguration Equation ((27), for non-norm conserving intensity shifts, but which are not solutions of the real reconfiguration equation (Equation (38).

[9] In the relativistic case, E_G^{Di} has to be replaced by $\frac{d}{d\bar{\tau}} S_G^{Di}(\bar{\tau}_{_C})$ (cf. Equations 35 and 33).

Detector 1 leads to reconfigurations to State 1 or to Bundle ¬1, i.e. a superposition of State 2 and 3. The competitions for spacetime geometry at the locations of the other two detectors lead to four further reconfigurations accordingly. The two reconfigurations corresponding to the competition between State 2 and Bundle ¬2 on the location of Detector 2 are illustrated in Figure 10, where the upper part of the figure shows the reconfiguration of the wavefunction's evolution in configuration space, and the lower part the corresponding behaviour in spacetime. When the system reduces to a superposition of States 1 and 3, as shown on the right in Figure 10, this superposition will reduce at a later reduction point in time $\bar{t}_{C}$ to one of the states, which is given by $S_G^{D1}(\bar{t}_{C})+S_G^{D3}(\bar{t}_{C})=\hbar$.

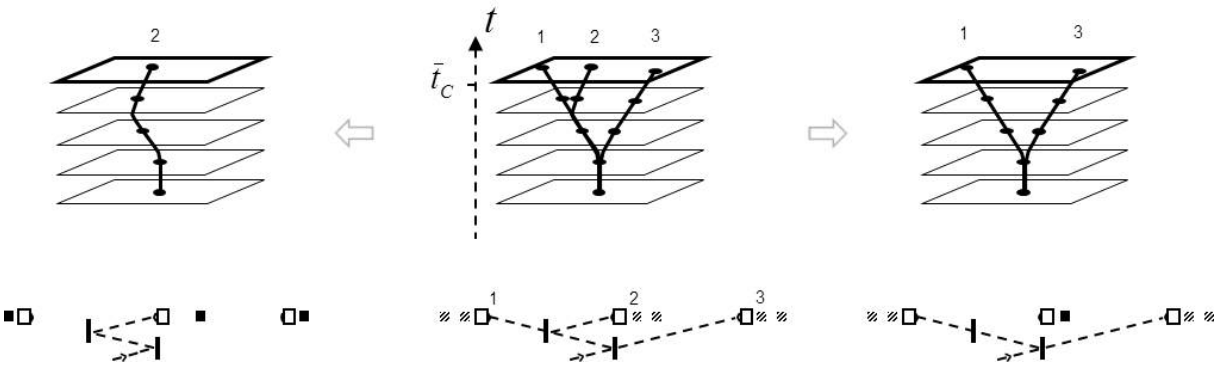

Fig. 10: Two possible reconfigurations of the wavefunction's evolution in configuration space for the three-detector experiment in Figure 8 (upper part) and corresponding behaviour in spacetime (lower part) according to the discussion in the text.

How a photon localises when measured by a film

With our results, we can discuss how a photon localises when it is measured by a film, as in Figure 9. Here the initial superposition of N states reduces at the reduction point in time $\bar{t}_{C}$ when the sum of the detectors' local competition actions reaches Planck's quantum of action ($\sum_j S_G^{Dj}(\bar{t}_{C})=\hbar$) with a low probability directly to a state i, and a high one to a superposition $\neg i$. In the latter case, the superposition $\neg i$ decays at a later point in time $\bar{t}_{C\neg i}$, which is given by $\sum_{j\neq i} S_G^{Dj}(\bar{t}_{C\neg i})=\hbar$, again with a low probability to a single state, and a high one to a superposition of $N-2$ states. This procedure repeats at subsequent reduction points in time, until the superposition has reduced to a single state i, and the photon has localised at one of the detectors.

The initial superposition of N states can decay in many different ways to the same final state i. With the reconfiguration rule (Equation 44), according to which the decay probability to a bundle is proportional to the bundle's intensity, one can easily see how the probability of all ways leading to a final state i follows Born's rule, i.e.

$$p_i = I_i \quad . \qquad \textit{Born's rule} \tag{45}$$

10 Deviations from Born's rule

In this section we search for regimes for which the Dynamical Spacetime approach predicts possible deviations from Born's rule. These regimes must have (according to our analysis of typical quantum mechanical experiments in Section 9) more than two local bundles on one bundle area. In the experiment in Figure 11, the solid on the right is transferred into a three-state superposition, where Detector 1 displaces the solid by Δs_{01}, and Detector 2 by Δs_{02}, as shown in the figure. The reduction probabilities of such a regime with three local bundles will be investigated now.

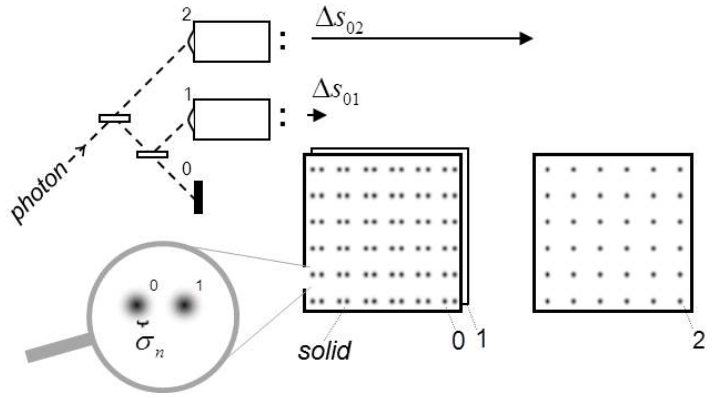

Fig. 11: Experiment for transferring a solid into a three-state superposition. For photon detection, Detectors 1 and 2 displace the solid by Δs_{01}, respectively Δs_{02}.

Diósi-Penrose energies

To simplify discussion, we assume that the displacement between States 0 and 2 Δs_{02} is much larger than that between State 0 and 1 Δs_{01}, as shown in Figure 11. Since the Diósi-Penrose energy between rigid bodies E_{Gij} increases typically with the square of the distance between the bodies ($E_{Gij} \propto \Delta s_{ij}^2$; see e.g. [3]), the Diósi-Penrose energies between the three states of the solid can be approximated by

$$\begin{matrix} E_{G02} \approx E_{G12} \equiv E_G \\ E_{G01} \approx 0 \end{matrix} \quad . \tag{46}$$

Reconfiguration equation

When the displacements Δs_{01} and Δs_{02} are approximately constant over time, the competition actions between the states are given by $S_{Gij}(\bar{t}) = E_{Gij}\bar{t}$. The reconfiguration equation (Equation 38) then leads to

$$\begin{pmatrix} dI_0 \\ dI_1 \\ dI_2 \end{pmatrix} = \frac{E_G \bar{t}}{\hbar} \begin{pmatrix} I_2 & 0 & -I_0 \\ 0 & I_2 & -I_1 \\ -I_2 & -I_2 & (I_0 + I_1) \end{pmatrix} \begin{pmatrix} dI_0 \\ dI_1 \\ dI_2 \end{pmatrix} \quad . \quad \textit{reconfiguration equation} \tag{47}$$

The smallest dynamical parameter $\bar{t}$ for which this equation allows for intensity shifts $d\vec{I}$ is

$$\bar{t}_{C} = \frac{\hbar}{E_{G}} \quad , \qquad \textit{reduction point in time} \tag{48}$$

and the corresponding reconfiguration solutions $d\vec{I}_{C}$ are

$$d\vec{I}_{C} \propto \begin{pmatrix} -I_{0} \\ -I_{1} \\ I_{0}+I_{1} \end{pmatrix} \quad , \qquad \textit{reconfiguration solutions} \tag{49}$$

which span a one-dimensional solution space.

Reconfiguration rule

According to the discussion in Section 8.4, the intensity vector $\vec{I}$ can reconfigure to $\vec{I}'_{+}=\vec{I}+\hat{\alpha}_{+}d\vec{I}_{C}=(0,0,1)^{T}$ or to $\vec{I}'_{-}=\vec{I}-\hat{\alpha}_{-}d\vec{I}_{C}=\frac{1}{I_{0}+I_{1}}(I_{0},I_{1},0)^{T}$, which are State 2 or a superposition of States 0 and 1. This is the intuitively expected result for a small displacement Δs_{01} between States 0 and 1, where the superposition of States 0 and 1 does not differ much from a single state. The decay-trigger rates of the states follow with Equations (34) and (32) as:

$$\begin{aligned} \frac{dp_{0\downarrow}}{d\bar{t}} &= \frac{I_{1}E_{G01}+I_{2}E_{G02}}{\hbar} \quad \approx \quad I_{2}\frac{E_{G}}{\hbar} \quad \textit{with} \;\; dI_{C0}<0 \\ \frac{dp_{1\downarrow}}{d\bar{t}} &= \frac{I_{0}E_{G01}+I_{2}E_{G02}}{\hbar} \quad \approx \quad I_{2}\frac{E_{G}}{\hbar} \quad \textit{with} \;\; dI_{C1}<0 \quad , \qquad \textit{decay-trigger rates} \\ \frac{dp_{2\downarrow}}{d\bar{t}} &= \frac{I_{0}E_{G02}+I_{1}E_{G12}}{\hbar} \approx (I_{0}+I_{1})\frac{E_{G}}{\hbar} \quad \textit{with} \;\; dI_{C2}>0 \end{aligned} \tag{50}$$

where the decay-triggers of States 0 and 1 have a negative, and the decay-trigger of State 2 a positive, projection on the reduction solution $d\vec{I}_{C}$. This leads to the following reconfiguration rule (cf. Equation 40):

$$\begin{pmatrix} I_{0} \\ I_{1} \\ I_{2} \end{pmatrix} \rightarrow \begin{cases} \begin{pmatrix} 0 \\ 0 \\ 1 \end{pmatrix} & \textit{with} \;\; p_{2} \propto 2I_{2}\dfrac{E_{G}}{\hbar} \\ \\ \frac{1}{I_{0}+I_{1}}\begin{pmatrix} I_{0} \\ I_{1} \\ 0 \end{pmatrix} & \textit{with} \;\; p_{01} \propto (I_{0}+I_{1})\dfrac{E_{G}}{\hbar} \end{cases} . \qquad \textit{reconfiguration rule} \tag{51}$$

With the normalisation of the reduction probabilities $p_{2}+p_{01}=1$ and $I_{0}+I_{1}+I_{2}=1$, we obtain the following reduction probability of State 2:

$$p_{_2} = \frac{2}{1 + I_{_2}} I_{_2} \ , \tag{52}$$

which is for $I_{_2} = \frac{1}{4}$ a factor of 1.6 larger than that predicted by Born's rule ($p_{_2}{=}I_{_2}$).

Why State 2's reduction probability is increased

The increased reduction probability of State 2 with respect to Born's rule can be explained as follows. According to Equation (50), States 0 and 1 have the same decay-trigger rates, since they both suffer approximately the same energy increase in the mean gravitational potential of the superposition. This decay-trigger rate is identical to that of the single state, which one obtains by merging States 0 and 1 ($\Delta s_{01}{\to}0$). Since States 0 and 1 trigger both a reconfiguration to State 2 (cf. Equation 50), one obtains a doubling of the decay-trigger rate in favour of State 2 with respect to the case that States 0 and 1 are merged, which explains the increased reduction probability of State 2 with respect to Born's rule. The transition of the increased reduction probability of State 2 of $p_{_2}{=}2I_{_2}/(1{+}I_{_2})$ back to Born's rule ($p_{_2}{=}I_{_2}$) for $\Delta s_{01}{\to}0$ can be explained by the physical argument that the decay-trigger rates of States 0 and 1 must be correlated when they are merged into one state. Then they cannot be counted twice in the reconfiguration rule. This raises the question of the physical criterion for the decorrelation of the decay-trigger rates of States 0 and 1.

Decorrelation criterion

The decay-trigger rates of States 0 and 1 are expected to be decorrelated when their mass distributions are disjoint. The mass distribution of a solid's nuclei can be approximated by Gaussian distributions like $\rho(\mathbf{x}){\propto}exp(-\mathbf{x}^2/(2\sigma_n^2))$, where σ_n is the spatial variation of the nuclei, as shown in Figure 11, which is typically on the order of a tenth of an Ångström [3]. The mass distributions of States 0 and 1 are disjoint when the displacement Δs_{01} between them is at least six times larger than the spatial variation of their nuclei σ_n:

$$\Delta s_{01}(\bar{t}_{_C}) > 6\sigma_n \ . \qquad \textit{decorrelation criterion} \tag{53}$$

To observe the increased reduction probability of State 2, this so-called *decorrelation criterion* has to be satisfied at the reduction point in time of the superposition $\bar{t}_{_C}$.

For the derivation of the decorrelation criterion, it is important to recapitulate the conclusion at the end of Section 8.4, that the reconfiguration probabilities depend only on the states' decay-trigger rates, and not on their intensities determining the amplitudes of the decay-triggers, which play no role in the self-reinforcing reconfiguration mechanism of the Dynamical Spacetime approach. When we increase the displacement between States 0 and 1 from $\Delta s_{01}{=}0$ to $\Delta s_{01}{>}6\sigma_n$, the superposition of States 0 and 1 can be compared to one state having twice as many nuclei as the merged state of

States 0 and 1 ($\Delta s_{01}=0$) and half of the intensity as this state. The doubling of nuclei doubles the state's decay-trigger rate (since it doubles its energy increase), and the halving of its intensity only reduces the amplitudes of its decay-triggers, which plays no role. The doubling of the state's decay-trigger rate displays the decorrelation of State 0's and 1's decay-trigger rates according to the decorrelation criterion for $\Delta s_{01}>6\sigma_n$.

One might wonder why State 2's reduction probability $p_2=2I_2/(1+I_2)$ does not depend on the intensities of States 0 and 1. This is also due to the fact that these intensities only determine the amplitudes of the states' decay-triggers, but not their decay-trigger rates.

—

Completeness of the model

In this section, we ask how far the so-far specified model for the Dynamical Spacetime approach is complete. Our model is sufficient for a discussion of the typical quantum mechanical experiments, as shown in Section 9, and for a discussion of concrete experiments for checking deviations from Born's, as will be shown in [4]. An open issue remains: how to model the transition between cases, where we can characterise the competition for spacetime geometry by local competition actions, such as in the three-detector experiment in Figure 8, or by "global" competition actions, such as in the experiment in Figure 11, where as solid is transferred into a three-state superposition. In this case, the integrals of the competition actions must not be restricted to the location of the solid, which therefore can be regarded as "global" competition actions. If one calculates the experiment in Figure 8 with three "global" competition actions S_{G12}, S_{G13} and S_{G23} (measuring the competition of the three classical scenarios for the spacetime geometry on whole spacetime) instead of the three local ones S_G^{D1}, S_G^{D2} and S_G^{D3}, one obtains a different result. Since there is a smooth transition between the experiment in Figure 8 and that in Figure 11 in the way that the three detectors in Figure 8 change mass distributions on their locations, and the detectors in Figure 11 on a common location, how to model the transition remains an open issue.

11 Signalling

In this section, we discuss the physical consequences resulting from deviations from Born's rule. Since some proofs for the impossibility of superluminal signalling refer to Born's rule [64, 65], and vice versa (some derivations of Born's rule refer to the no-signalling argument [61, 62]), it is not surprising that deviations from Born's rule imply the possibility of superluminal signalling.

A signalling experiment can be constructed by modifying an EPR experiment, as shown in Figure 12. The setup places Bob in position to manipulate the ratio between the polarisation probabilities measured by Alice from usually $p_{H}/p_{V}=1$ to $p_{H}/p_{V}=2$ by removing the aperture, which allows a solid evolve into a three-state superposition, as shown in the figure. This result follows with Equation (52) for $I_{2} = \frac{1}{2}$ and a Bell state of $|\psi>=|H>|H>+|V>|V>$. This enables Bob to signal information to Alice. To ensure that the superposition is reduced by Bob's apparatus, Alice's arm must be chosen to be at least $c\bar{t}_{C}$ longer than Bob's.

This prediction of superluminal signalling does not provoke a conflict with relativity, since causality evolves in the Dynamical Spacetime approach orthogonal to spacetime, as explained in the discussion of quantum correlations in Section 6.

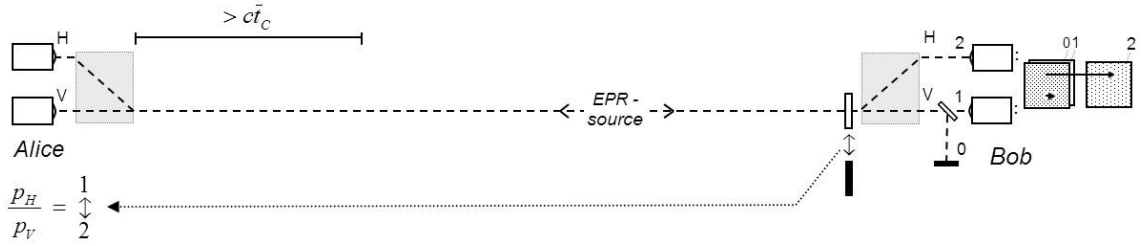

Fig. 12: Signalling experiment in which Bob can manipulate the ratio between the polarisation probabilities measured by Alice from usually $p_{H}/p_{V}=1$ to $p_{H}/p_{V}=2$ by removing the aperture.

12 Energy conservation

In this section, we investigate how far the Dynamical Spacetime approach conserves energy.

In the Dynamical Spacetime approach, total energy is conserved on average, as illustrated in Figure 13. The behaviour shown in Figure 13 can be explained as follows. From the analysis of semiclassical gravity in Part 1 [1], it follows that the total energy of a two-state superposition ($|\psi>=c_1|\psi_1>+c_2|\psi_2>$) can be decomposed as

$$E = |c_1|^2 E_1 + |c_2|^2 E_1 + |c_1|^2|c_2|^2 E_{G12} \ , \tag{54}$$

where E_1 and E_2 are the total energies of States 1 and 2 alone (i.e. referring to the case that they must not share spacetime geometry with the other state), and E_{G12} the Diósi-Penrose energy. The energies E_1 and E_2 of States 1 and 2 are constant over time ($E_i(t)=const$), since they refer to classical trajectories at which the State does not share spacetime geometry with the other state and resides in its own gravitational potential. With this result and $|c_1|^2 + |c_2|^2 = 1$, Equation (54) can be transformed to

$$E(t) = E(t_s) + |c_1|^2|c_2|^2 E_{G12}(t) \ , \tag{55}$$

where t_s is the point in time at which the superposition is generated. At collapse, at which one of the intensities $|c_1|^2$ or $|c_2|^2$ vanishes, total energy falls from $E(t_s)+|c_1|^2|c_2|^2 E_{G12}(\bar{t}_C)$ back to $E(t_s)$, the energy before the superposition was generated. This is the behaviour illustrated in Figure 13. The energy increase before the collapse of $|c_1|^2|c_2|^2 E_{G12}(\bar{t}_C)$ follows from the sharing of spacetime geometry in semiclassical gravity.

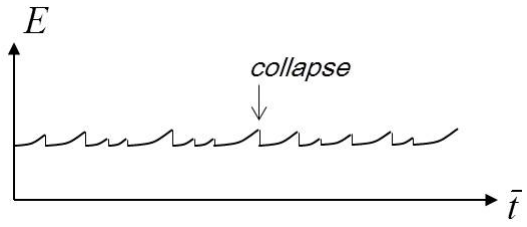

Fig. 13: Behaviour of total energy over time in the Dynamical Spacetime approach.

The behaviour of total energy in the Dynamical Spacetime approach is different to that in dynamical reduction models, in which total energy permanently increases due to the introduction of stochastically fluctuating operators [28] [10]. Spontaneous photon emissions, which could be a consequence of this permanent energy increase, as discussed elsewhere [66–69], are not expected in the Dynamical Spacetime approach.

[10] In recent publications, modifications of the dynamical reduction models have been proposed, through which the permanent energy increase can be avoided [70, 71].

13 Ontology

In this section, we discuss the ontology of the Dynamical Spacetime approach. The question of ontology plays an important role for the assessment of collapse models. For the dynamical reduction models, the so-called matter density and flash ontologies have been established [72–75]. The question of ontology is challenging especially for relativistic collapse models [29,30,34,74], in which one is free to choose the reference frame.

Matter density ontology
The Dynamical Spacetime approach allows for the definition of a matter density ontology. For each expansion of spacetime, the wavefunction's evolution on spacetime until the spacetime border can be determined unambiguously and independently from the chosen reference frame with the Tomonaga-Schwinger equation [54,55], and by taking a boundary condition on the spacetime border into account. The energy momentum tensor field, respectively the matter density, follows from the wavefunction with the help of suitable operators.

Ontology of collapse
In the Dynamical Spacetime approach, collapse is only possible at specified points in time: the reduction points in time $\bar{t}_C$. This is different to the dynamical reduction models, in which collapse is (due to the introduction of a stochastic process) possible at any point in time. This allows us to define an ontology for the collapse event, which is specified by the critical position of spacetime border $\bar{\tau}_C$ and the corresponding change of matter density at this point in time. In the dynamical reduction models, it is unclear whether the collapse event itself is something objective. In [76], it is shown that one cannot accurately measure the number of collapses that a given physical system undergoes during a given time interval.

In the context of ontology, the questions are of interest as to whether the Dynamical Spacetime approach's postulate (the existence of the spacetime border), and its most important prediction (collapse events being only possible at specified points in time), can be checked by experiments. We will now discuss these issues.

Measurement of the spacetime border
If one assumes that the spacetime border's propagation started at the Big Bang singularity and spread around this singularity symmetrically, as illustrated in Figure 14, it should be observable in a today's experiment as a plain hypersurface, whose propagation direction depends on the relative motion of the experimenter's reference frame to the cosmos. This propagation direction can be measured with the signalling experiment in Figure 12 by systematically varying the lengths of Alice's and Bob's arms, as shown in Figure 15. This leads to regimes in which Bob cannot signal information towards Alice, when the spacetime border hits Alice's measurement first, as shown on the right in Figure 15.

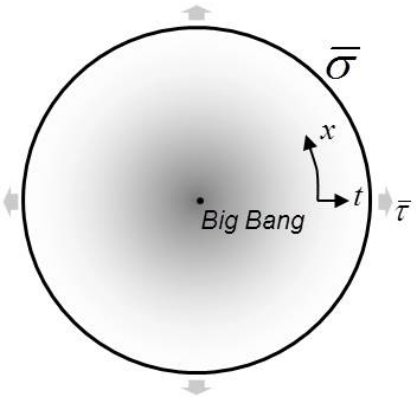

Fig. 14: Dynamical expansion of the spacetime border $\bar{\sigma}$ around the Big Bang singularity.

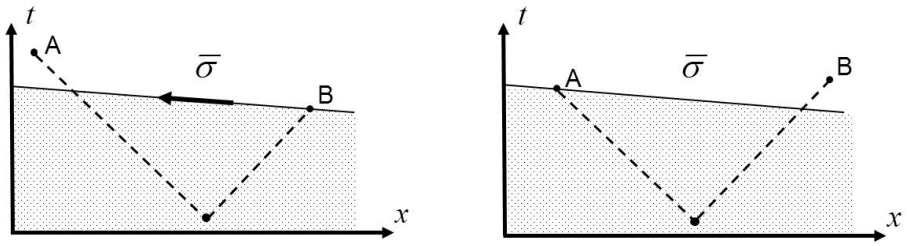

Fig. 15: Illustration of measurement of the propagation direction of the spacetime border by varying the lengths of the arms of the signalling experiment in Figure 12. When the spacetime border hits Alice's measurement first, as on the right, Bob cannot signal information to Alice.

Measurement of collapse events

The most important prediction of the Dynamical Spacetime approach that collapse is only possible at specified points in time $\bar{t}_C$ and that the lifetimes of superpositions correspond to the ones of the gravity-based approaches of Diósi and Penrose can also be checked by experiments.

If one allows the solid in Figure 11 first evolve into a two-state superposition by delaying the displacement between States 0 and 1 Δs_{01} by a time delay of Δt, one observes an increased reduction probability of State 2 only, when the two-state superposition has not reduced before Δt. By measuring the reduction probability of State 2 over the time delay Δt, one can determine the reduction point in time $\bar{t}_C$ (of the two-state superposition), and check whether collapse is only possible at a specified point in time: the reduction point in time $\bar{t}_C$. In [4], it is shown how such an experiment can be realised.

14 Towards a Dynamical Spacetime theory

In this section, we discuss how the Dynamical Spacetime approach could be promoted towards a Dynamical Spacetime theory. Such a theory should address the expansion of spacetime instead of postulating it. This should lead to an equation of motion for the propagation of the spacetime border, which must be Lorentz invariant.

One option for such a theory is to describe the existence of the spacetime border by a dynamical metrical field $g_{\mu\nu}(x, \bar{\tau})$, whose factor of the covariant volume element breaks down on the spacetime border, i.e. $\sqrt{-g(x, \bar{\tau})} \approx 0$ for $x > \bar{\sigma}(\bar{\tau})$. This ensures that the Einstein-Hilbert action only accounts until the spacetime border, as assumed in the Dynamical Spacetime approach. Such a program requires an enhancement of Einstein's field equations for dynamical metric fields. The solutions to the enhanced field equations should describe the expansion of spacetime and lead to an equation of motion for the propagation of the spacetime border $\bar{\sigma}(\bar{\tau})$. An interesting question is whether such a program could be completed without introducing further natural constants.

Another interesting theoretical question is whether the Dynamical Spacetime approach can address the divergence problem of quantum field theory.

15 Discussion

The Dynamical Spacetime approach to wavefunction collapse is a new way to combine quantum theory with general relativity with the capability of explaining the known facts about wavefunction collapse, such as the quantum correlations and Born's rule. The Dynamical Spacetime postulate, which looks at first glance an ad-hoc hypothesis, can be considered as an answer to the question that the concept of spacetime necessarily provokes. Do spacetime regions, in which future events will happen, already exist today? The assumption that the spacetime regions, in which future events will happen, are dynamically created also explains, why advanced potentials (such as e.g. in electrodynamics) must be left out. The Dynamical Spacetime postulate introduces our subjective experience of present, past and future into the concept of spacetime, where the present can be considered as the spacetime region before the spacetime border, in which collapse events happen.

The most important result of the Dynamical Spacetime approach is its capability to explain collapse by the quasi-abrupt reconfigurations of the wavefunction's evolution at specified critical expansions of spacetime displaying both the stochastic and the non-local nature of collapse, in a natural way. Collapse's stochastic nature follows from the critical positions of spacetime border at which the smallest fluctuations decide in favour of which state the wavefunction's evolution reconfigures. This makes the introduction of a stochastic process by hand, or to say it in the words of Einstein the assumption that "God plays dice", superfluous. Collapse's non-local nature follows from the quasi-abrupt reconfigurations of the wavefunction's evolution, which can cover far-separated spacetime regions. The fact that these configurations always incorporate the complete history of a superposition (i.e. from the splitting of the wavepacket in configuration space) makes how quantum correlations can follow the predictions of quantum theory comprehensible. The quasi-abrupt reconfigurations of the wavefunction's evolution at collapse are based on a local causality occurring along the wavepackets' paths in configuration space. They are an explanation for the "spooky action at a distance", which even Einstein might have accepted, since the principle of only local causality is not abandoned.

The second important result of the Dynamical Spacetime approach is its capability to forecast reduction probabilities and the relation between Born's rule and semiclassical gravity. The Dynamical Spacetime approach is the first approach that can forecast reduction probabilities, and does not fear the consequences of deviations from Born's rule in the form of superluminal signalling. The discussion of typical quantum mechanical experiments revealed the common property of these experiments: that they generate never more than two different mass distributions at one location. This result shows where to seek new effects, such as for solids in three-state superpositions.

The surprise of the Dynamical Spacetime approach is the prediction of superluminal signalling. That there could be something faster than light is implicitly predicted by the Free Will Theorem. To discuss this explicitly still taboo, which is displayed by a statement that John Bell made in an interview shortly before his death [77]:

that maybe there must be something happening faster than light, although it pains me even to say that much.

John S. Bell

This taboo results from the fear that a faster-than-light causality places the well-established principle of relativity in question. The Dynamical Spacetime approach shows that this must not be the case. The result that the abrupt reconfigurations of the wavefunction's evolution can cover far-away spacetime regions shows how the deep and troubling conflict between relativity and quantum theory can be overcome.

In [4], an experiment for checking the predicted deviations from Born's rule for solids in three-state superpositions is proposed. The feasibility of the experiment is shown by a detailed quantitative analysis, which is based on the collapse model derived here; and a formulary for the Diósi-Penrose criterion for solids in quantum superpositions, which is derived in [3], but whose study is not essential [4]. The analyses in [4] show that deviations from Born's rule can only be observed in specially designed experiments, which explains why deviations from Born's rule have not become conspicuous so far.

Acknowledgements
I would like to thank my friend Christoph Lamm for supporting me and for proofreading the manuscript.

Appendix

In this appendix, we derive Equation (11) of how the intensity of a path reacts to changes of its detuning action. Due to the boundary condition at the spacetime border at $\bar{t}$, the frequencies of the wavepacket's partial waves can only increase in the discrete steps $\Delta\omega = n \cdot \pi/T$, with $T = \bar{t} - t_s$. The expectation value of n depends on the detuning action of the path dS_G as $<n> = dS_G/(\pi\hbar)$ ($dS_G = \hbar <\Delta\omega> T$). Assuming a Poisson distribution, i.e. $\sigma_n = \sqrt{<n>}$, we obtain for the spectral broadening of the wavepacket σ_ω with $\sigma_\omega = \sigma_n \cdot \pi/T$ the following estimate:

$$\sigma_\omega = \sqrt{\frac{\pi dS_G}{\hbar}} \frac{1}{T} \quad . \tag{56}$$

The spectral broadening of the wavepacket leads via the divergence of phases of its partial waves to the following decrease of intensity over time [11]:

$$I_\rightarrow(t) = \left| \int_\infty^{-\infty} d\omega \frac{1}{\sqrt{2\pi}\sigma_\omega} e^{-\frac{\omega^2}{2\sigma_\omega^2}} e^{i\omega(t-t_s)} \right|^2 = e^{-\sigma_\omega^2 (t-t_s)^2} \ . \tag{57}$$

This result cannot be correct, since due to the norm conservation of unitary evolution, the intensity of the wavepacket must be constant along the path. If we assume that the boundary condition on the spacetime border at $\bar{t}$ leads to a reflected wave with an intensity profile of $I_\leftarrow = e^{-\sigma_\omega^2 (t-\bar{t})^2}$, we obtain an approximately constant intensity along the path. The intensity drop of the path is then given by [12]

$$I' = \frac{1}{2T} \left(\int_{t_s}^{\bar{t}} dt I_\rightarrow(t) + \int_{t_s}^{\bar{t}} dt I_\leftarrow(t) \right) \approx 1 - \frac{\pi}{3} \frac{dS_G}{\hbar} \approx 1 - \frac{dS_G}{\hbar} \ , \tag{58}$$

which leads to Equation (11) ($dI/I = -dS_G/\hbar$). That this result displays Equation (11) only approximately ($\pi/3 \approx 1$) is probably related to the fact that the intensity profile of our calculation ($I(t) = I_\rightarrow(t) + I_\leftarrow(t)$) is only approximately constant over time.

[11] Equation (57) follows with $\int_{-\infty}^{\infty} dx e^{-a^2x^2} cos(bx) = \frac{\sqrt{\pi}}{a} e^{-\frac{b^2}{4a^2}}$ [78].

[12] $I_\rightarrow(t) \approx 1 - \sigma_\omega^2 t^2$.

References

[1] ***G. Quandt-Wiese***, Towards a theory of wavefunction collapse Part 1: How the Diósi-Penrose criterion and Born's rule can be derived from semiclassical gravity and how the Diósi-Penrose criterion can be relativistically generalised with the help of the Einstein-Hilbert action, *arXiv:1701.00343 (2017)*

[2] ***G. Quandt-Wiese***, The Dynamical Spacetime approach to wavefunction collapse in a nut-shell, *http://quandt-wiese.de/onewebmedia/DynamicalSpacetimeApproach.pdf*

[3] ***G. Quandt-Wiese***, Diósi-Penrose criterion for solids in quantum superpositions and a single-photon detector, *arXiv:1701.00353 (2017)*

[4] ***G. Quandt-Wiese***, Experimental proposal for the Dynamical Spacetime approach to wave-function collapse, *arXiv:1701.00355 (2017)*

[5] ***D. Bohm, B. J. Hiley***, *Phys. Rev., 85, 166 (1952)*

[6] ***D. Bohm, B. J. Hiley***, The Undivided Universe: an Ontological Interpretation of Quantum Theory, *Routledge, London (1993)*

[7] ***P. Pearle***, Might God toss coins?, *Found. Phys., 12, 249-63 (1982)*

[8] ***P. Pearle***, Stochastic dynamical reduction theories and superluminal communication, *Phys. Rev. D, 33, 2240-52 (1986)*

[9] ***G. C. Ghirardi, A. Rimini, T. Weber***, Unified dynamics for microscopic and macroscopic systems, *Phys. Rev. D, 34, 470-91 (1986)*

[10] ***G. C. Ghirardi, P. Pearle, A. Rimini***, Markov processes in Hilbert space and continuous spontaneous localization of systems of identical particles, *Phys. Rev. A, 42, 78-89 (1990)*

[11] ***R.P. Feynman***, Lectures on gravitation, *Caltech, place (1962)*

[12] ***L. Diósi***, Models for universal reduction of macroscopic quantum fluctuations, *Phys. Rev. A, 40, 1165-1174 (1989)*

[13] ***R. Penrose***, On gravity's role in quantum state reduction, *Gen. Rel. Grav., 28, 581-600 (1996)*

[14] ***W. Marshall, C. Simon, R. Penrose, D. Bouwmeester***, Towards quantum superpositions of a mirror, *Phys. Rev. Lett., 91, 130401 (2003), arXiv:quant-ph/0210001*

[15] ***J. van Wezel, T. Oosterkamp, J. Zaanen***, Towards an experimental test of gravity-induced quantum state reduction, *Phil. Mag., 88, 1005 (2008), arXiv:0706.3976*

[16] ***S. Bose, K. Jacobs, P. L. Knight***, Scheme to probe the decoherence of a macroscopic object, *Phys. Rev. A, 59, 3204-3210 (1999), arXiv:quant-ph/9712017*

[17] ***O. Romero-Isart***, Quantum Superposition of Massive Objects and Collapse Models, *Phys. Rev. A, 84, 052121 (2011), arXiv:1110.4495*

[18] ***M. Ho, A. Lafont, N. Sangouard, P. Sekatski***, Probing wave function collapse models with a classically driven mechanical oscillator, *New J. Phys., 18, 033025 (2016), arXiv:1504.00790*

[19] ***J. Christian***, Testing gravity-driven collapse of the wavefunction via cosmogenic neutrinos, *Phys. Rev. Lett., 95, 160403 (2005), arXiv:quant-ph/0503001*

[20] ***D. Salart, A. Baas, J. A.W. van Houwelingen, N. Gisin, H. Zbinden***, Spacelike Separation in a Bell Test Assuming Gravitationally Induced Collapses, *Phys. Rev. Lett., 100, 220404 (2008), arXiv:0803.2425*

[21] ***A. Bassi, K. Lochan, S. Satin, T. P. Singh, H. Ulbricht***, Models of Wave-function Collapse, Underlying Theories, and Experimental Tests, *Rev. Mod. Phys., 85, 471-527 (2013) arXiv:1204.4325*

[22] ***K. Münch-Berndl, D. Dürr, S. Goldstein, N. Zanghi***, Nonlocality, Lorentz invariance, and Bohmian quantum theory, *Phys. Rev. A, 53, 2062-2073 (1996), arXiv:quant-ph/0303156*

[23] ***T. M. Salmos***, Bohmian Mechanics and Quantum Theory, *J. Stat. Phys., 80, 793 (1995)*

[24] ***D. Dürr, S. Goldstein, K. Münch-Berndl, N. Zanghi***, Hypersurface Bohm-Dirac models, *Phys. Rev. A, 60, 2729-2736 (1999), arXiv:quant-ph/9801070*

[25] ***H. Nikolic***, Relativistic-covariant Bohmian mechanics with proper foliation, *arXiv:1205.4102 (2012)*

[26] ***D. Dürr, S. Goldstein, T. Norsen, W. Struyve, N. Zanghi***, Can Bohmian mechanics be made relativistic?, *Proc. R. Soc. A , 470, 20130699 (2014), arXiv:1307.1714*

[27] ***G. C. Ghirardi***, Interpretation of quantum mechanics: where do we stand?, *Jour. of Phys., 174, 012013 (2009), arXiv:0904.0958*

[28] ***A. Bassi, G. C. Ghirardi***, Dynamical Reduction Models, *Phys. Rept., 379, 257 (2003), arXiv:quant-ph/0302164*

[29] ***G. C. Ghirardi, R. Grassi, P. Pearl***, Relativistic Dynamical Reduction Models: General Framework and Examples, *Found. Phys., 20, 1271-1336 (1990)*

[30] ***G. C. Ghirardi***, Local Measurements of Nonlocal Observables and the Relativistic Reduction Process, *Found. Phys., 30, 1337-1385 (2000), arXiv:quant-ph/0003149*

[31] ***C. Dove, E. J. Squires***, Symmetric Versions of Explicit Wavefunction Collapse Models, *Found. Phys., 25, 1267-1282 (1995)*

[32] ***T. M. Samols***, A Stochastic Model of Quantum Field Theory, *Jour. Stat. Phys., 80, 793-809 (1995), arXiv:hep-th/9501117*

[33] ***R. Tumulka***, On Spontaneous wave function collapse and quantum field theory, *Proc. R. Soc. A, 462, 1897-1908 (2006), arXiv:quant-ph/0508230*

[34] ***R. Tumulka***, A Relativistic Version of the Ghirardi-Rimini-Weber Model, *Found. Phys., 125, 825-844 (2006), arXiv:quant-ph/0406094*

[35] ***D. J. Bedingham***, Relativistic State reduction dynamics, *Found. Phys., 41, 686-704 (2010), arXiv:1003.2774*

[36] ***F. Dowker, I. Herbauts***, The Status of the Wave Function in Dynamical Collapse Models, *Found. Phys. Lett., 18, 499-518 (2005), arXiv:quant-ph/0411050*

[37] ***P. Pearle***, A Relativistic Dynamical Collapse Model, *arXiv:1412.6723 (2014)*

[38] ***J. Conway, S. Kochen***, The Free Will Theorem, *Found. Phys., 36, 1441-1473 (2006), arXiv:quant-ph/0604079*

[39] ***J.H. Conway, S. Kochen***, The Strong FreeWill Theorem, *Notices of the American Math. Soc., 56, 226 (2009), arXiv:0807.3286*

[40] ***A. Bassi, G. Ghirardi***, The Conway-Kochen Argument and Relativistic GRW Models, *Found. Phys., 37, 169-185 (2007), arXiv:quant-ph/0610209*

[41] ***J. Conway, S. Kochen***, Reply to Comments of Bassi, Ghirardi, and Tumulka on the Free Will Theorem, *Found. Phys., 37, 1643-1647 (2007), arXiv:quant-ph/0701016*

[42] ***R. Tumulka***, Comment on "The Free Will Theorem", *Found. Phys., 37, 186-197 (2007), arXiv:quant-ph/0611283*

[43] ***N. Gisin***, The Free Will Theorem, Stochastic Quantum Dynamics and True Becoming in Relativistic Quantum Physics, *arXiv:1002.1392 (2010)*

[44] ***L. Rosenfeld***, *Nucl. Phys., 40, 353 (1963)*

[45] ***C. Møller***, *in Les Theories Relativistes de la Gravitation, Colloques Internationaux CNRS 91, edited by A. Lichnerowicz and M.-A. Tonnelat, CNRS, Paris (1962)*

[46] ***M. Bahrami, A. Großardt, S. Donadi, A. Bassi***, The Schrödinger-Newton equation and its foundations, *New J. Phys., 16, 115007 (2014), arXiv:1407.4370*

[47] ***J. R. van Meter***, Schrödinger-Newton "collapse" of the wave function, *Class.Quant.Grav., 28, 215013 (2011), arXiv:1105.1579*

[48] ***R. Penrose***, On the Gravitization of Quantum Mechanics 1: Quantum State Reduction, *Found Phys., 44, 557-575 (2014)*

[49] ***S. Carlip***, Is Quantum Gravity Necessary?, *Class. Quant. Grav., 25, 154010 (2008), arXiv:0803.3456*

[50] ***M. Bahrami, A. Bassi, S. McMillen, M. Paternostro, H. Ulbricht***, Is Gravity Quantum?, *arXiv:1507.05733 (2015)*

[51] ***J. S. Bell***, Speakable and Unspeakable in Quantum Mechanics, 2nd ed., *Cambridge University Press, Cambridge (2004)*

[52] ***L. Diósi***, Intrinsic time-uncertainties and decoherence: comparison of 4 models, *Brazilian Journal of Physics, 35, 260-265 (2005)*

[53] See textbooks on general relativity, *e.g. H. Stephani, Allgemeine Relativitätstheorie, VEB Deutscher Verlag der Wissenschaften, Berlin (1980) , or T. Fließbach, Allgemeine Relativitätstheorie, Spektrum, Heidelberg (2003)*

[54] ***S. Tomonaga***, On a Relativistically Invariant Formulation of the Quantum Theory of Wave Fields, *Prog. Theo. Phys., 1, 27 (1946)*

[55] ***J. Schwinger***, *Phys. Rev., 74, 1439 (1948)*

[56] ***P. H. Eberhard***, Bell's Theorem without Hidden Variables, *Nuovo Cimento, 38B, 75-80 (1976)*

[57] ***P. H. Eberhard***, Bell's Theorem and the Different Concepts of Locality, *Nuovo Cimento, 46B, 392-419 (1978)*

[58] ***A. M. Gleason***, Measures on the closed subspaces of a Hilbert space, *J. Math. Mech., 6, 885 (1957)*

[59] ***D. Deutsch***, Quantum theory of probability and decisions, *Proc. Roy. Soc. London, A455, 3129 (1999), arXiv:quant-ph/9906015*

[60] ***W. H. Zurek***, Environment-assisted invariance, entanglement, and probabilities in quantum physics, *Phys. Rev. Lett., 90(12), 120404 (2003)*

[61] ***M. Schlosshauer, A. Fine***, On Zurek's derivation of the Born rule, *Found. Phys., 35(2), 197-213 (2005), arXiv:quant-ph/0312058*

[62] ***E. J. Gillis***, Causality, Measurement, and Elementary Interactions, *arXiv:1007.4608 (2010)*

[63] ***A. V. Nenashev***, Quantum probabilities from combination of Zurek's envariance and Gleason's theorem, *Physica Scripta T, 163, 014033 (2014), arXiv:1406.0138*

[64] ***K. A. Peacock***, The No-Signalling Theorems: A Nitpicking Distinction, *philpapers (philosophical research online), http://philpapers.org*

[65] ***C. Hewitt-Horsman***, An introduction to many worlds in quantum computation, *Found. Phys., 39(8) (2009), arXiv:0802.2504*

[66] ***P. Pearle, E. Squires***, Bound state excitation, nucleon decay experiments, and models of wave function collapse, *Phys. Rev. Lett., 73, 1-5 (1994)*

[67] ***W. Feldmann, R. Tumulka***, Parameter Diagrams of the GRW and CSL Theories of Wave Function Collapse, *J. Phys. A: Math. Theor., 45, 065304 (2012), arXiv:1109.6579*

[68] ***S. L. Adler, A. Bassi, S. Donadi***, On spontaneous photon emission in collapse models, *Journ. Phys. A: Math. Theor., 46, 245304 (2013), arXiv:1011.3941*

[69] ***A. Bassi, S. Donadi***, Spontaneous photon-emission from a non-relativistic free charged particle in collapse models: A case-study, *Phys. Lett. A, 378, 761-765 (2014), arXiv:1307.0560*

[70] ***A. Smirne, A. Bassi***, Toward an energy-conserving model of spontaneous wavefunction collapse, *arXiv:1408.6446v1 (2014)*

[71] ***M. Bahrami, A. Smirne, A. Bassi***, Gravity and the Collapse of the Wave Function: a Probe into Diósi-Penrose model, *Phys. Rev. A, 90, 062105 (2014), arXiv:1408.6460*

[72] ***V. Allori, S. Goldstein, R. Tumulka, N. Zanghi***, Predictions and Primitive Ontology in Quantum Foundations: A Study of Examples, *British Journal for the Philosophy of Science, 65, 323-352 (2014), arXiv:1206.0019*

[73] ***R. Tumulka***, Paradoxes and Primitive Ontology in Collapse Theories of Quantum Mechanics, *arXiv:1102.5767 (2011)*

[74] ***D. Bedingham, D. Dürr, G. Ghirardi, S. Goldstein, R. Tumulka, N. Zanghi***, Matter Density and Relativistic Models of Wave Function Collapse, *Journal of Statistical Physics, 154, 623-631 (2014), arXiv:1111.1425*

[75] ***M. Esfeld, N. Gisin***, The GRW flash theory: a relativistic quantum ontology of matter in space-time?, *arXiv:1310.5308 (2013)*

[76] ***C. W. Cowan, R. Tumulka***, Epistemology of Wave Function Collapse in Quantum Physics, *British Journal for the Philosophy of Science 67(2): 405-434 (2016), arXiv:1307.0827*

[77] ***C. Mann, R. Crease***, Interview with John S. Bell., *Omni, 84-121 (1988)*

[78] See mathematical books on integrals, *e.g. Bronstein, Semendjajew, Taschenbuch der Mathematik, Verlag Harri Deutsch, Frankfurt (1981)*